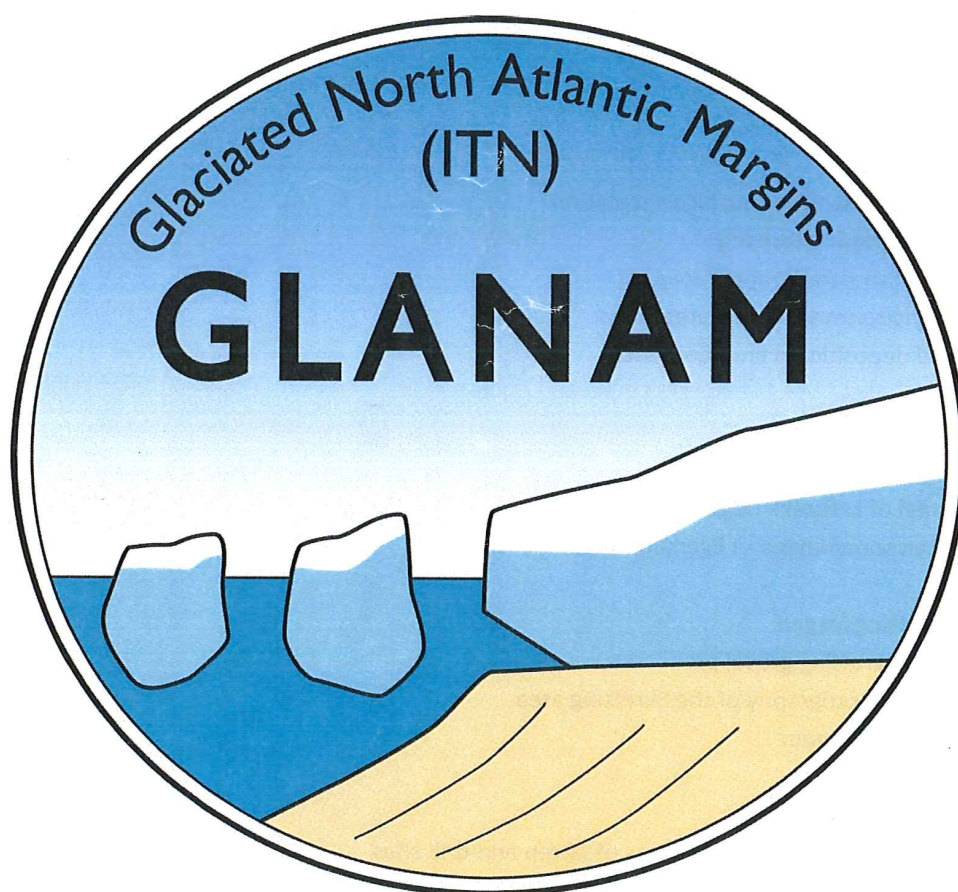


# Jæren Field Excursion Guide

led by Hans-Petter Sejrup  
&  
GLANAM Members



October 2013

## List of figures

### Day 1

	Page
1. Overview map	3
<b>Site 1 – Foss-Eikeland</b>	
2. Topographic map of Jæren area	4
3. Core logs (north – south profile)	5
4. Core logs (northwest – southeast profile)	6
5. Sedimentary facies of Figgjo gravel	7
6. Northern gravel pit	8
7. Geological evolution at Foss-Eikeland	9
<b>Site 2 – Jærmuseet Vitengarden</b>	
8. Nærbo location map and topography	10
9. Ice flow directions	11
<b>Site 3 - Grødaland</b>	
10. Location map with sea surface circulation	12
11. Lithostratigraphic core log	13
12. Modified lithostratigraphic core log	14
13. Palaeoenvironmental interpretations	15
14. Inferred depositional environments	16
<b>Site 4 – Lerbrekkvegen</b>	
15. Location of Norwegian Channel	17
16. 3D model of Lerbrekk ridge	18
17. Side-scan sonar image of Egersund Bank	19
<b>Site 5 – Skrettingsvegen</b>	
18. Profile of Skretting gravel pit	20
19. Composite stratigraphy of the Skretting area	21
20. Formation of sandur	22
<b>Site 6 – Elgane</b>	
21. Map showing morphological areas of Jæren and drill sites	23
22. Stratigraphies and amino acid values for Elgane and Auestad	24
23. Ice flow reconstruction	25
24. Map of western Norway and Norwegian Channel	26
25. Seismic interpretation of Norwegian Channel	27

### Day 2

26. Location of striations, fabric measurements and meltwater channels	28
27. Digital elevation model of Høggjæren Plateau	29
28. Ice dynamics during deglaciation	30
29. Radiocarbon dates from Jæren area	31
30. Ice extent during Last Glacial Maximum	32



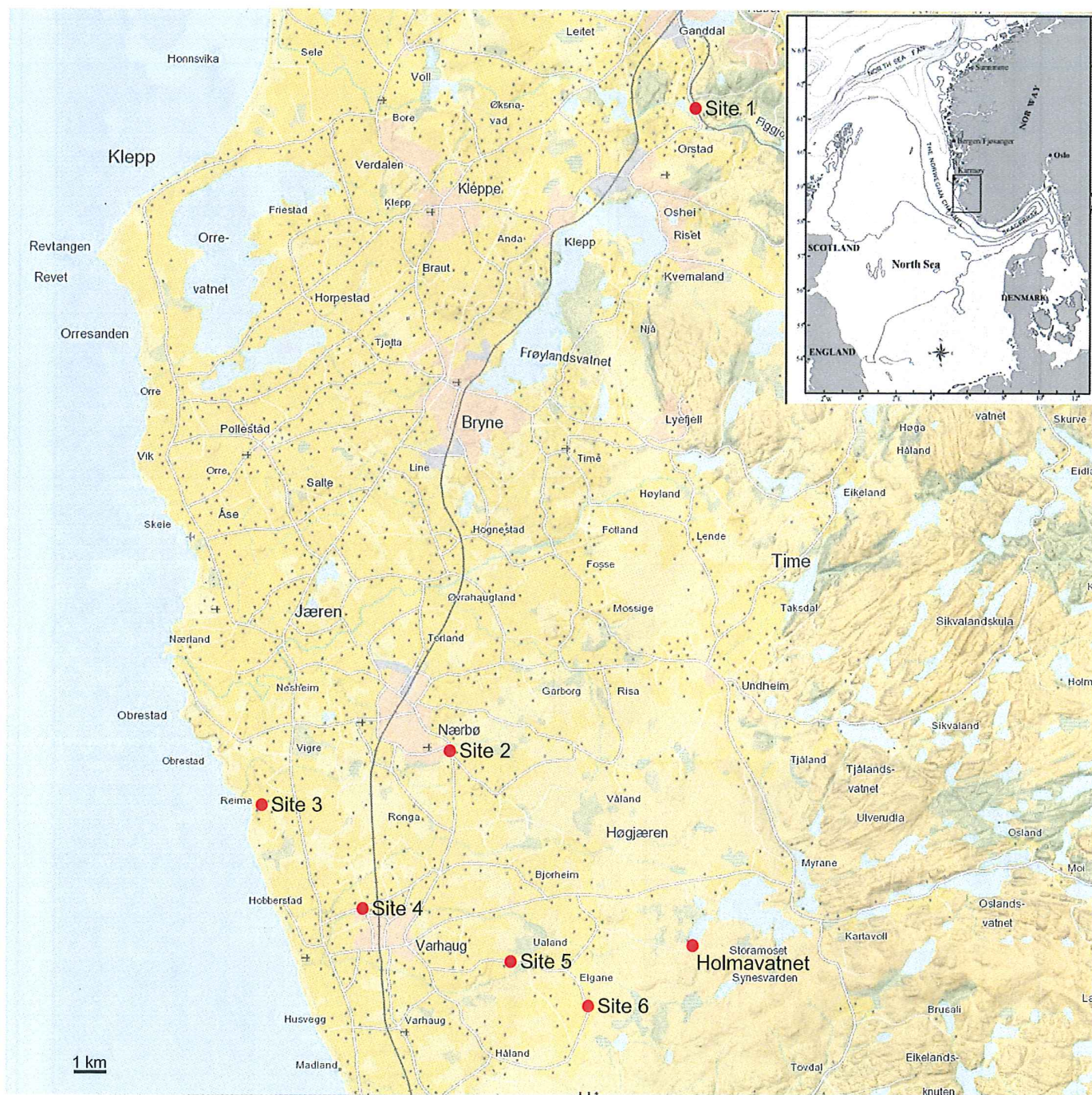


Figure 1. Location map with field sites



## Site 1: Foss-Eikeland

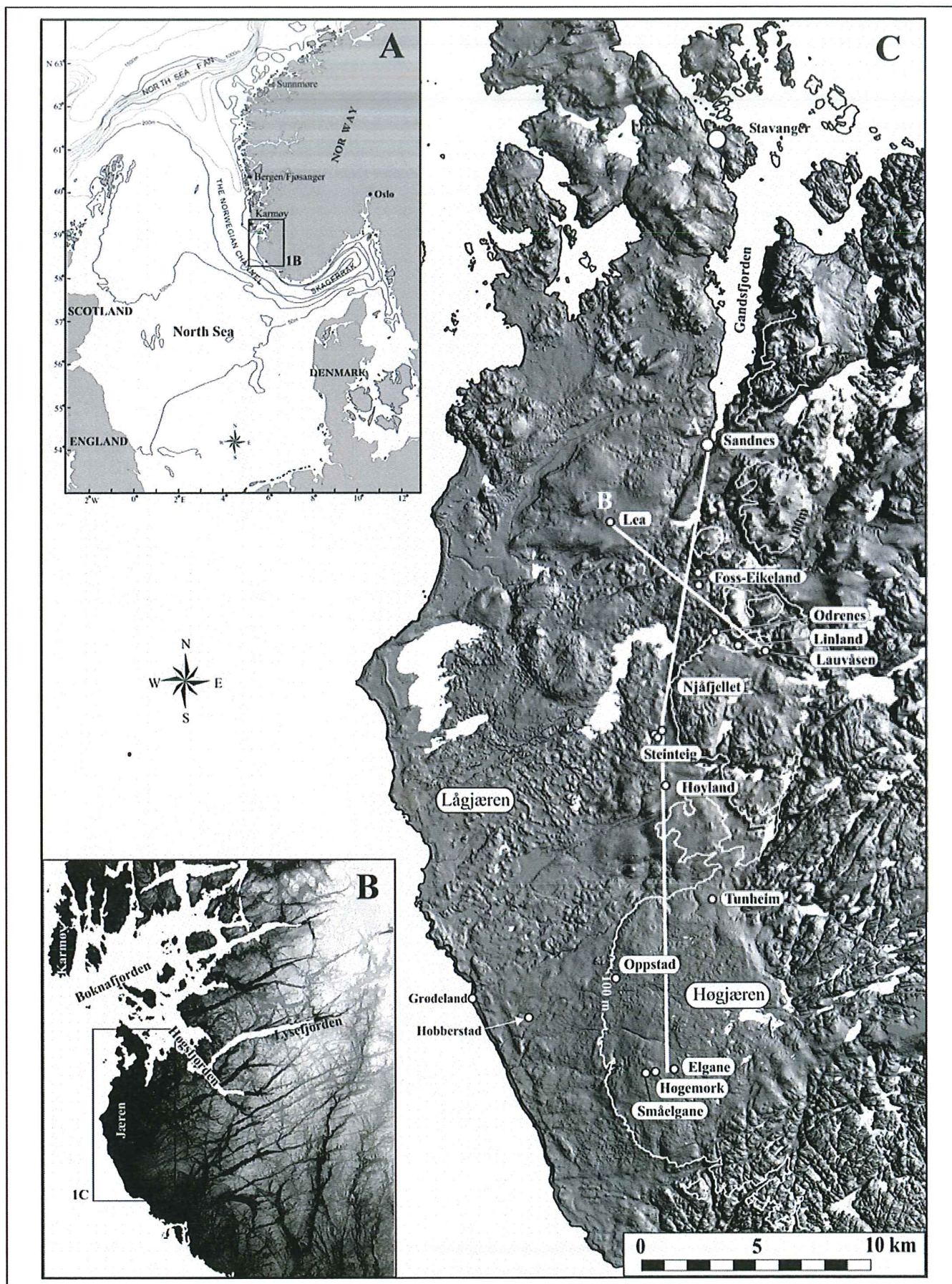


Fig. 2. A. Overview. B. Map of Rogaland, showing the orientation of valleys and fjords east and northeast of the Jæren area. C. Detailed map of Jæren presented as a 2D hill-shaded map with light from northeast. Sections have been investigated along two profiles. Profile A stretches from Sandnes in the north to Høgemork in the south, and profile B extends from Lea in the northwest to Lauvåsen in the southeast. From Raunholm et al. (2004).





Fig. 3 Logs from sections with glaciomarine sediments in a north-south profile at Jeren (profile A in Fig. 1C). For sections not described by the author, only interpretations of the sediments are shown. Note the different scales between the simplified logs and Fig. B-F. The stratigraphy at Sandnes (A) is from Feyling-Hanssen et al. (1971), Oppstad (G) is from Andersen et al. (1991), Smølgeane (H) is from Larsen et al. (2000), Elgane (I) is from Janocko et al. (1998) and Hogemork (J) is from Andersen et al. (1991). Not all previous publications have distinguished between laminated and homogeneous clay. Facies A and B are therefore marked by the same colour in the unit column. From Raunholm et al. (2004).



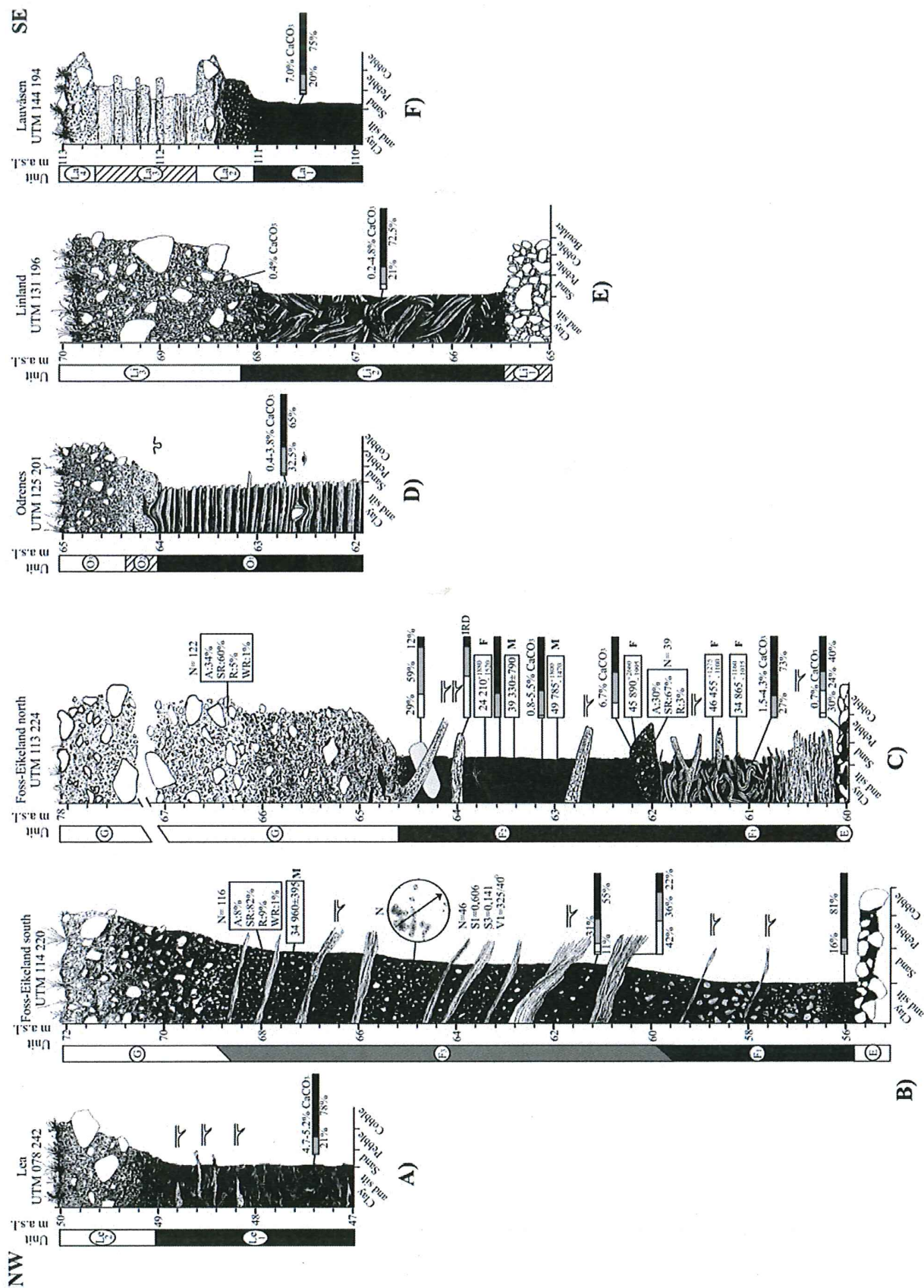
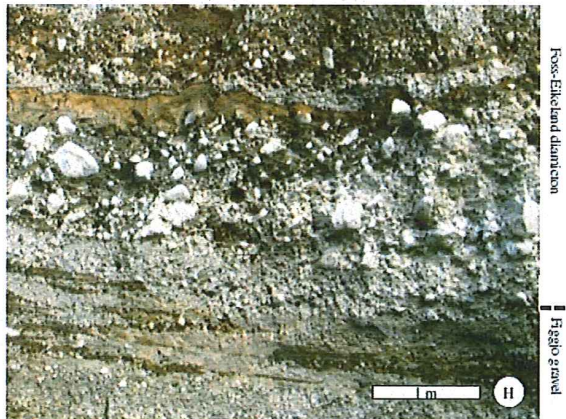
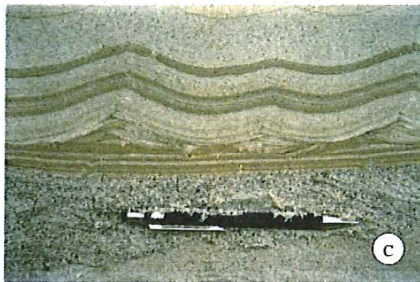
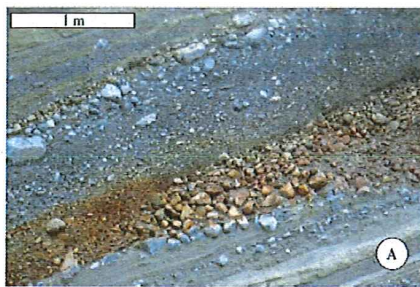


Fig. 4 Logs from sections with glaciomarine sediments in a northwest-southeast profile at Jæren (profile B in Fig. 1C). The logs from Foss-Eikeland (Figs. B & C) are modified from Raunholm et al. (2002). From Raunholm et al. 2004.





(A) open-work grainfall deposit (oxidized) overlain by inversely graded debris-flow deposits

(B) rhythmically laminated sand and silt interpreted as suspension deposits

(C) chevron cross-laminated ripples

(D) ripples climbing towards the east, against the general progradation direction of the delta

(E) fluid escape above the chevron ripples in (C)

(F) chute filled with normally graded pebbles and sand

(G) syngenetic ice-wedge cast in the middle part of subunit C<sub>2</sub>

(H) The contact between the Figgjo gravel and the Foss-Eikeland diamicton

**Figure 5** Sedimentary facies in subunit C<sub>1</sub>, the lower part of the Figgjo gravel (see Fig. 1 for location of 5a-h)  
Modified from Raunholm et al. (2002).



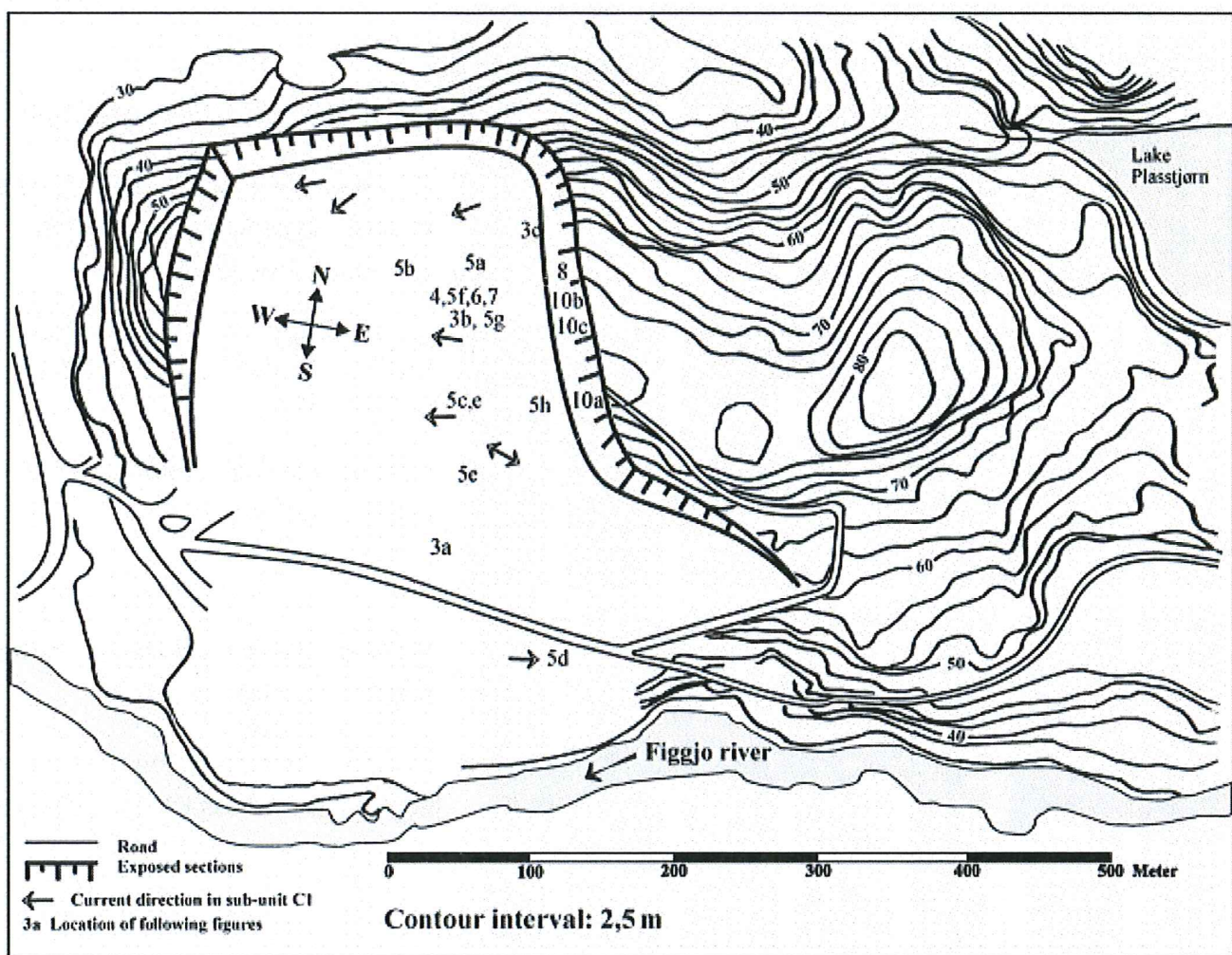


Fig. 6 The northern active gravel pit at Foss-Eikland. From Raunholm et al. (2002).



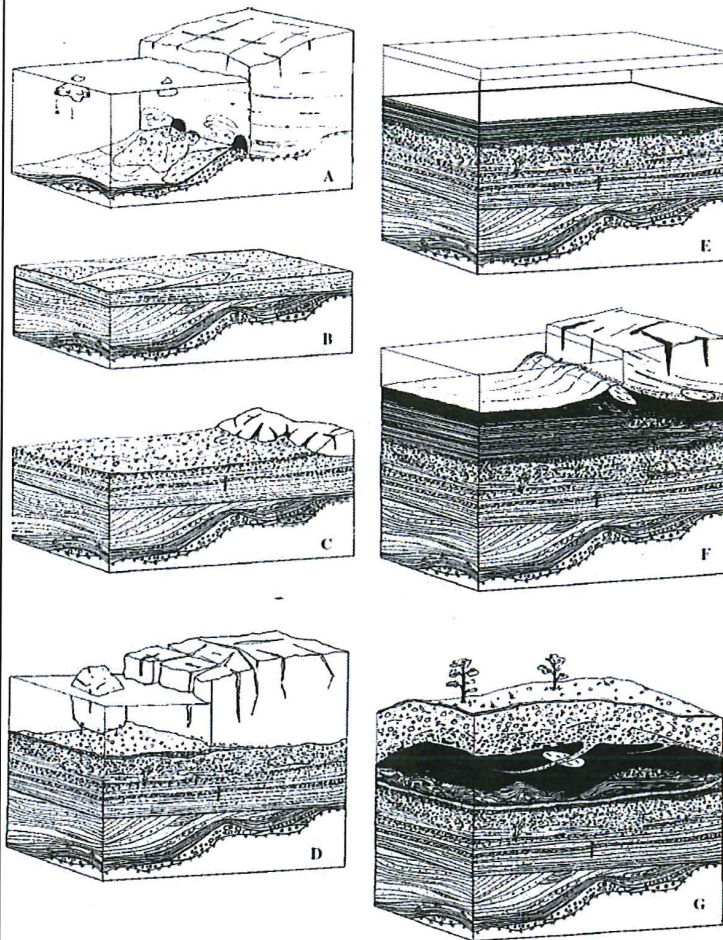
## Geological evolution at Foss-Eikeland

(A) deglaciation: coarse ice-contact fans, westwards fining of the sed., less outsized IRD; slumps, fluid & mollusc escape structures-> high sed. rate

(B) change from small to large epigenetic ice-wedge casts-> periods without sediment supply

(C) ice-proximal environment, stable or rising sea level

(D) wave and current erosion, grounded ice sheet in a submarine setting, Vagle boulder bed formation



(E) high relative sea level-> deposition of the lower part of Kalberg clay as a laminated facies

(F) glacial advance-> folding, faulting, brecciation

(G) deposition of Kverneland diamiction, a till deposited during the last advance of the Weichselian inland ice

The final deglaciation at Foss-Eikeland was terrestrial (marine limit <25m a.s.l. around here)

## Legend

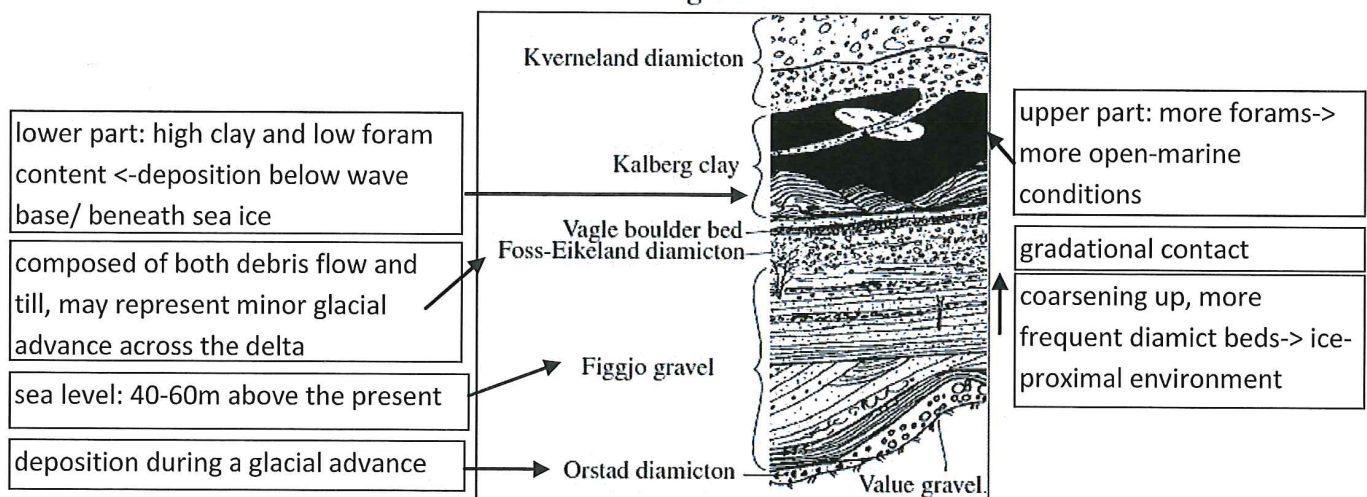


**Figure 7** Summary of the geological evolution at Foss-Eikeland. Modified from Raunholm et al. (2002).



## Site 2: Jærmuseet Vitengarden

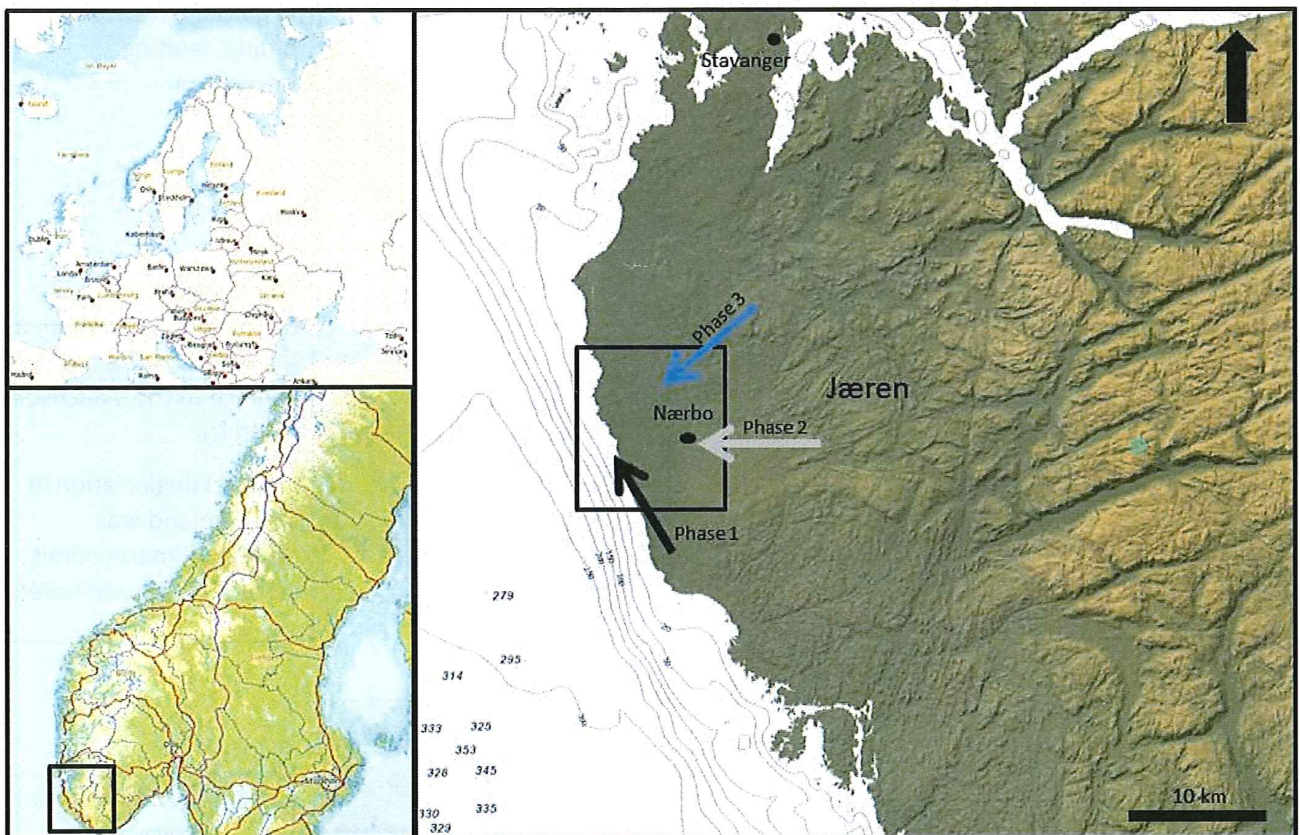


Fig. 8

Location of the study area. The arrows show three Late Weichselian ice-flow directions, with phase 1 showing the oldest ice flow direction. (Jonsdottir et al. 1999) Background maps from Norgeskart. From Jonsdottir et al. (1999).



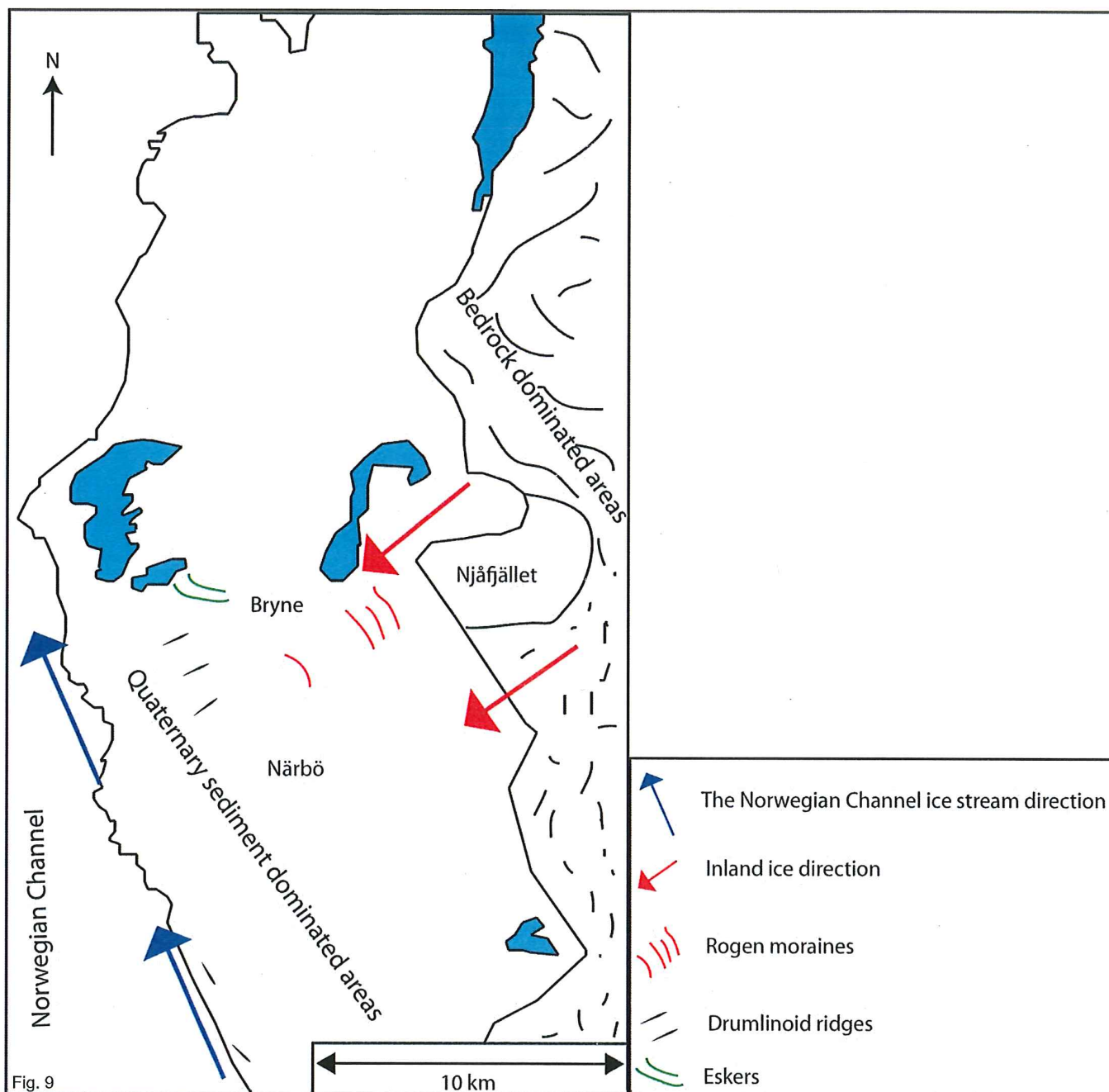


Fig. 9

The Jären area can be divided into a high-land bedrock area in the East and a low-land sediment dominated area in the West, which in turn borders to the Norwegian Channel. During LGM, while the Norwegian Channel was occupied by an ice stream (direction indicated by blue arrows), the Jären area was covered by inland ice (direction indicated by red arrows). The inland ice was feeding the ice stream, which is supported by the type and direction of several landforms in the Bryne/Närbö area. The final deglaciation of Jären took place around 13-14 ka BP. After Raunholm et al., 2003.



## Site 3: Grødalund

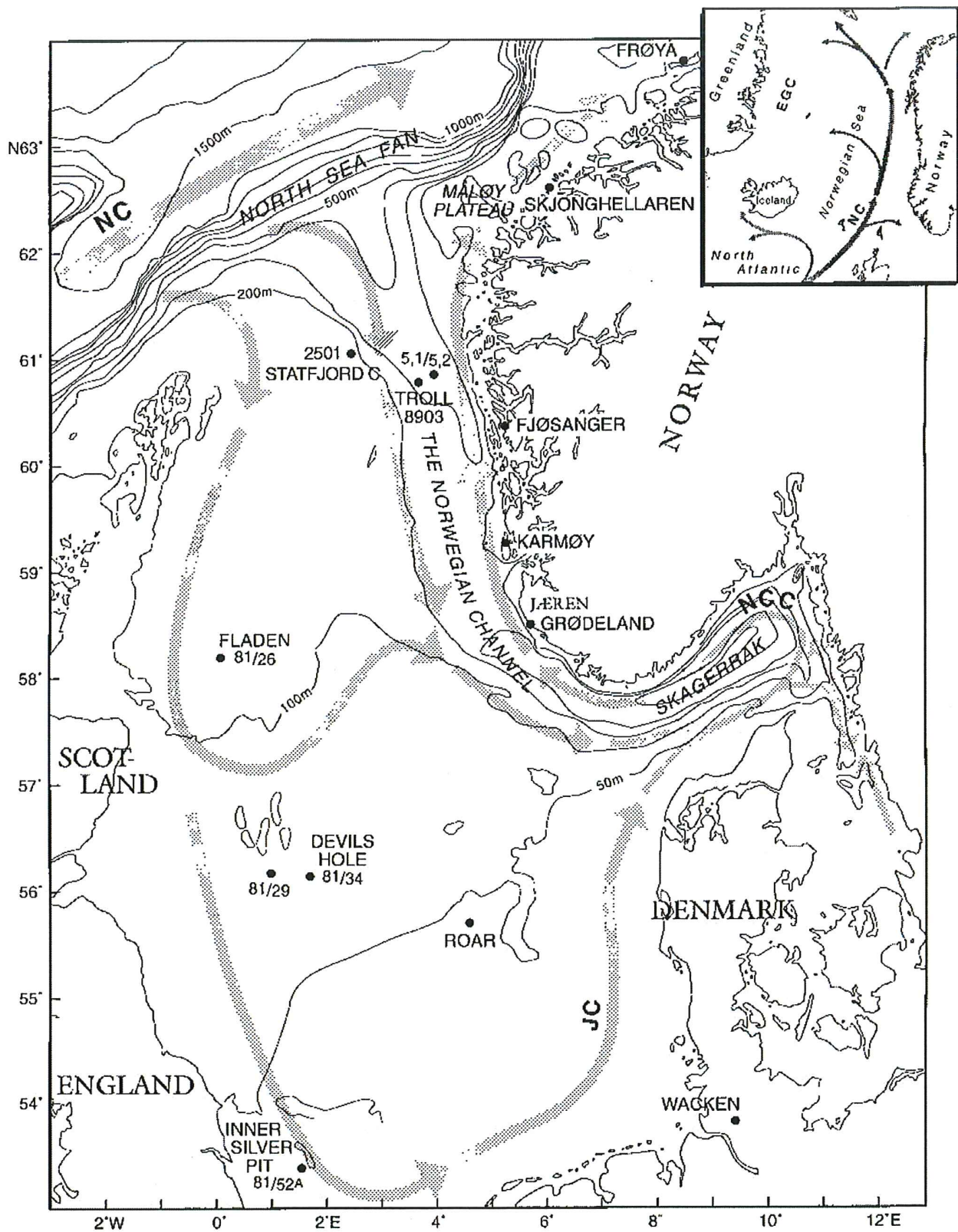


Fig. 10 Locations of the sites discussed in the text and the present surface circulation in the North Sea and the Nordic Seas. EGC = East Greenland Current, NC = Norwegian Current. JC = Jutland Current and NCC = Norwegian Coastal Current. From Sejrup et al. (1999).







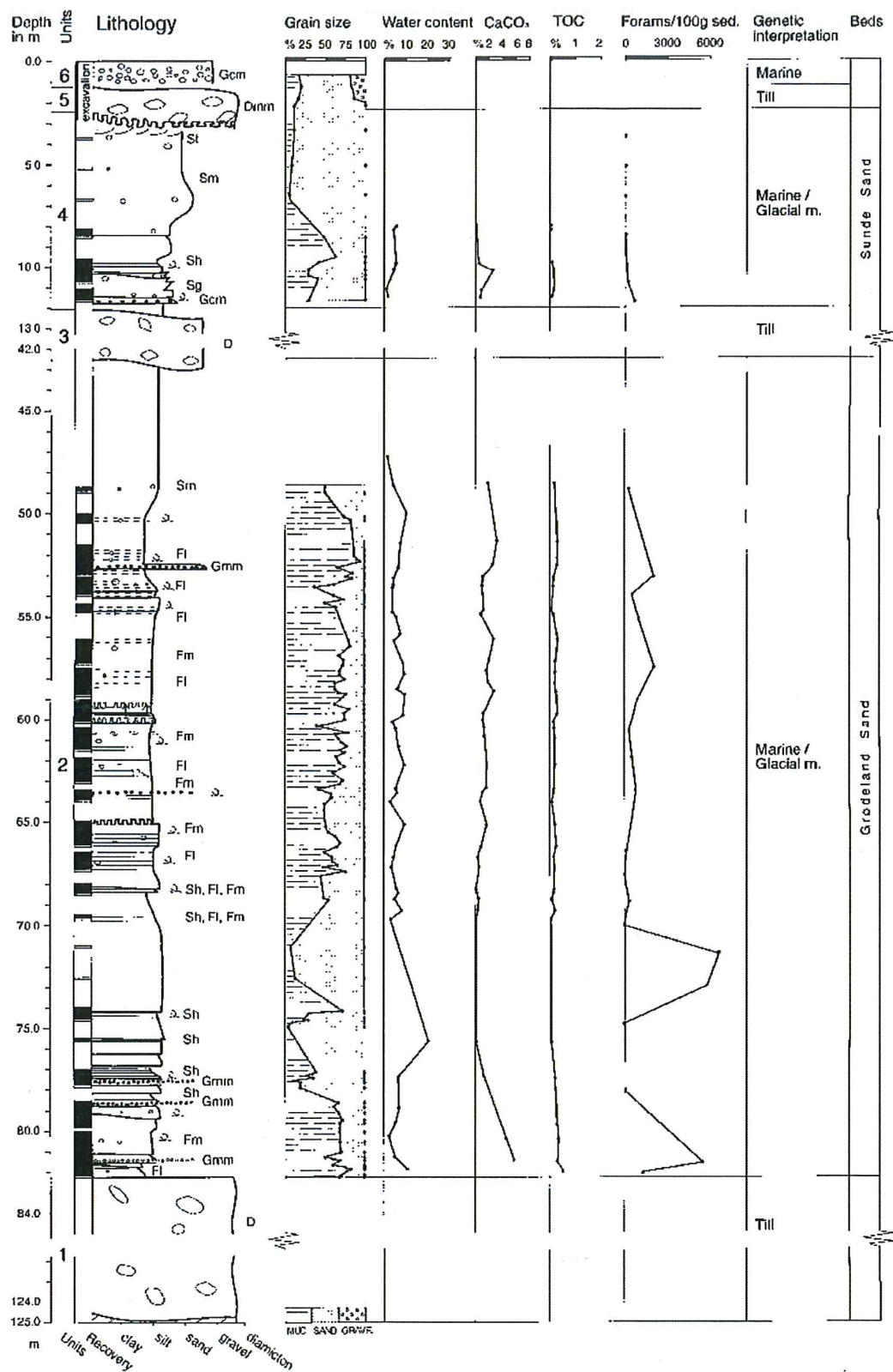


Fig.12 The lithostratigraphy of the Grødeland core. Note the break in depth scale in units 1 and 3. Facies codes are modified from Eyles (1983). Modified from Janocko *et al.* (1997).

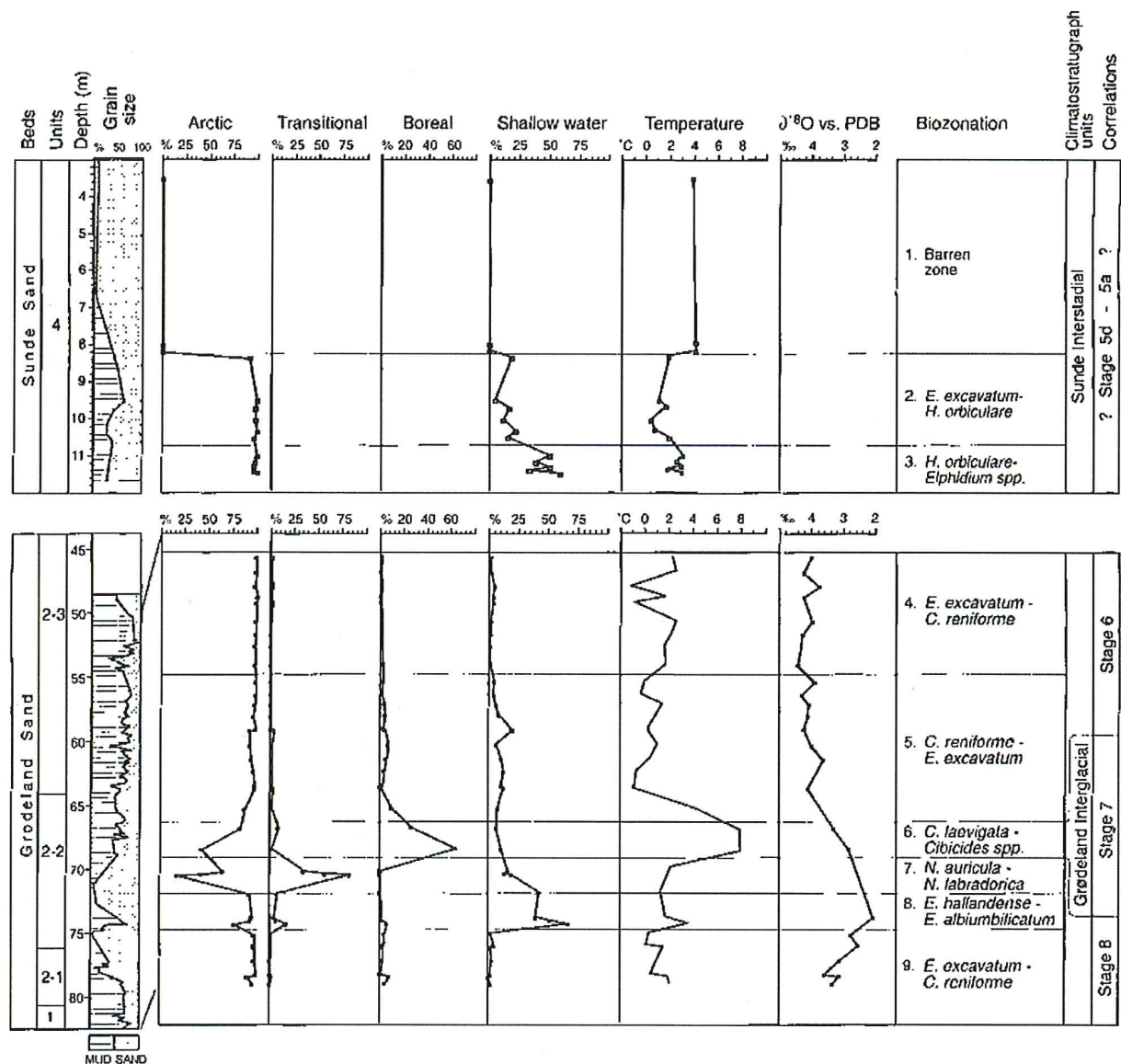


Fig.13 The Grødeland and Sunde interstadials. Percentages of the foraminiferal environmental groupings given in the Appendix. The temperature curve is based on the Poole *et al.* (1994) equation for all samples except for the two interglacial samples (Zone 6). The basis for the temperature estimate for the latter is given in the text. The 'mean' oxygen isotope curve (Fig. 5B) is also included. From Sejrup *et al.* (1999).



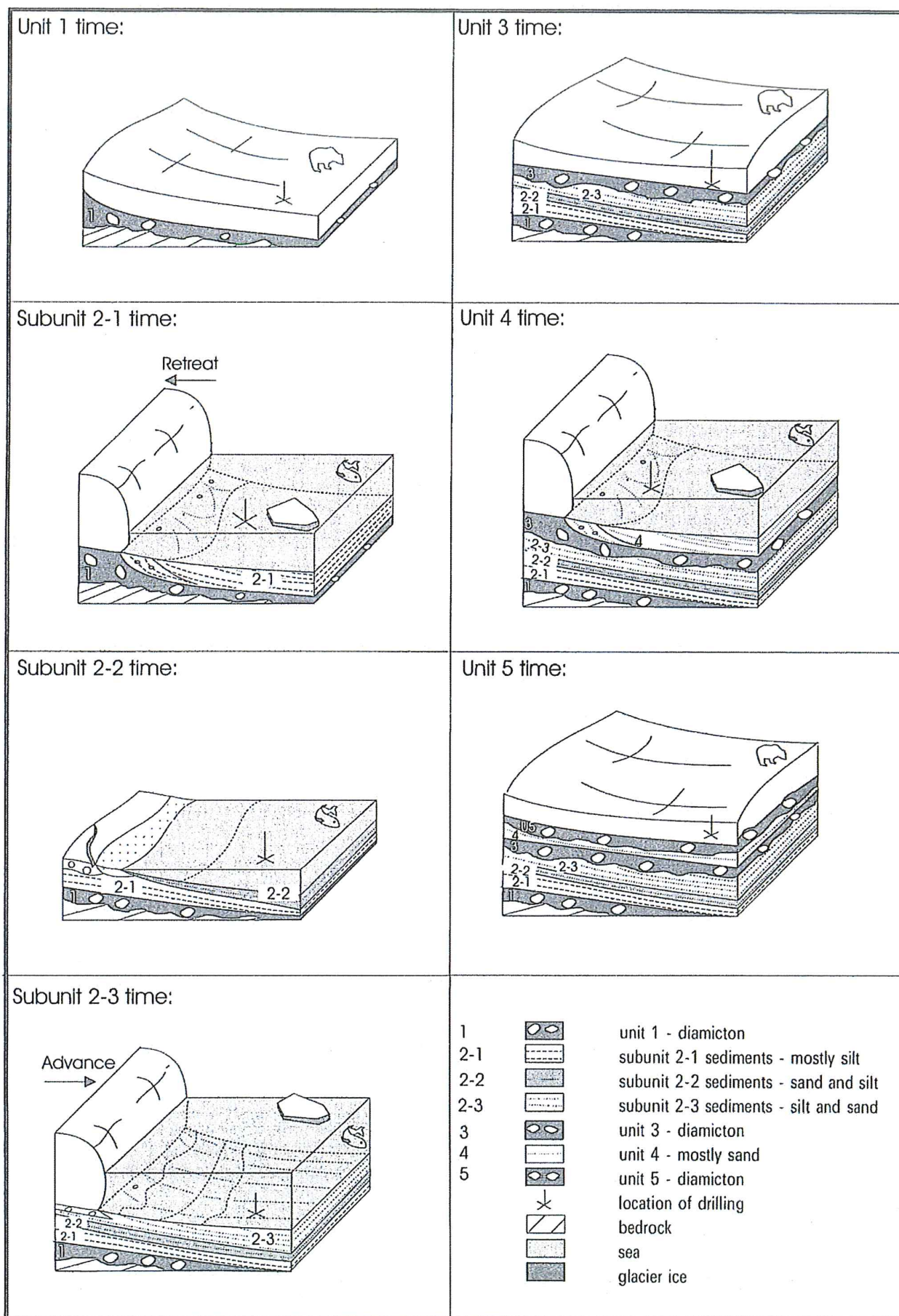


Fig. 14

Inferred depositional environments for the entire sedimentary sequence at Grødeland. Unit 1 time - deposition of till; subunit 2-1 time - glaciomarine sedimentation during glacier retreat; subunit 2-2 time - normal marine sedimentation in a storm-dominated environment; subunit 2-3 time - glaciomarine sedimentation of subunit 2-3 evolving from normal marine conditions; unit 3 time - glacial conditions, sedimentation of (at least) the lower part of unit 3; unit 4 time - glaciomarine sedimentation of unit 4; unit 5 time - glacial conditions, sedimentation of the uppermost till layer of unit 5 (Janocko et al., 1997).

## Site 4: Lerbrekkvegen

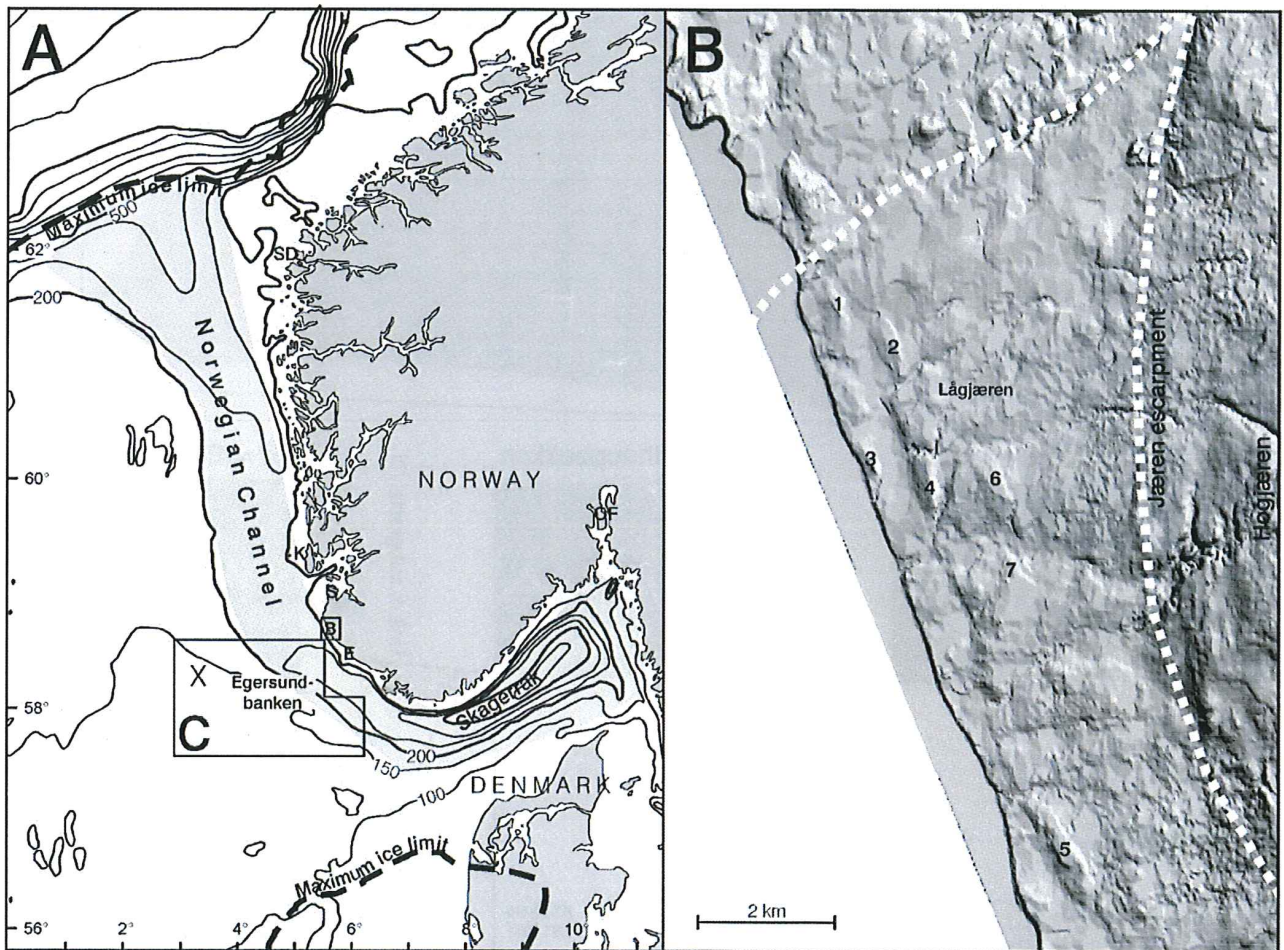


Fig.15 A. Location of the Norwegian Channel. Bathymetry contour interval 100 m. Ice limits after Sejrup *et al.* (1998). E = Egersund, K = Karmøy, OF = Oslofjorden, S = Stavanger and SD = Stad. B. Sun-shaded map of the study area of southern Lågjøren. Dashed lines indicate the borders to hummocky morphology to the north and the Jæren escarpment to the east. Morphological elements: 1-5 = drumlins parallel to the Norwegian Channel; 6 and 7 = drumlins oblique to both terrestrial ice and coastal ice stream; 4 = Lerbrekk. C. Area covered with side-scan sonar data, and Fig. 13 is located at 'X'. From Stalsberg *et al.* (2003).



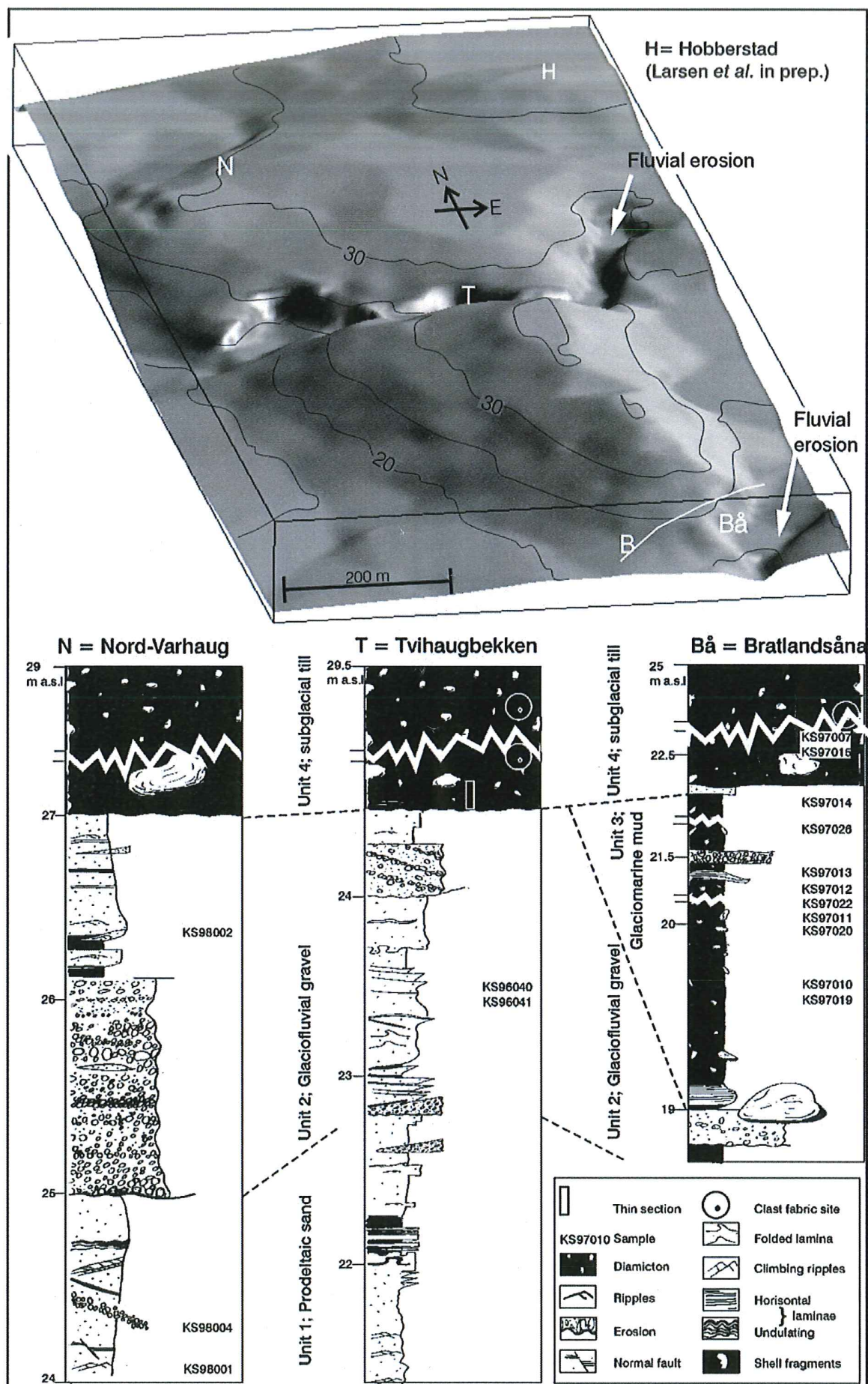
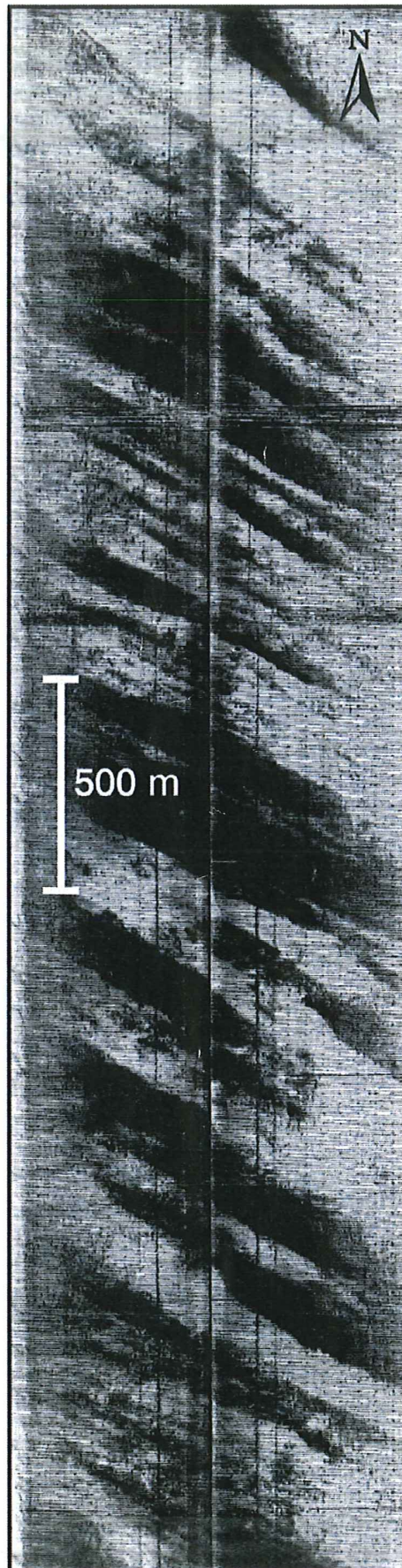


Fig. 16. 3D model of investigated Lerbrekk ridge with location of excavations. B=Bratland, location of trench marked with white line. Sampling sites are located on the logs. From Stalsberg *et al.* (2003).



*Fig.17* Side-scan sonar image of the sea bottom on the Egersund Bank in about 120 m of water depth. Dark linear elements trending northwest-southeast are interpreted as glacial megaflutes (ridges) related to the Norwegian Channel ice stream. Light areas indicate sand between the ridges (from Ottesen *et al.* 1999).



## Site 5: Skrettingsvegen

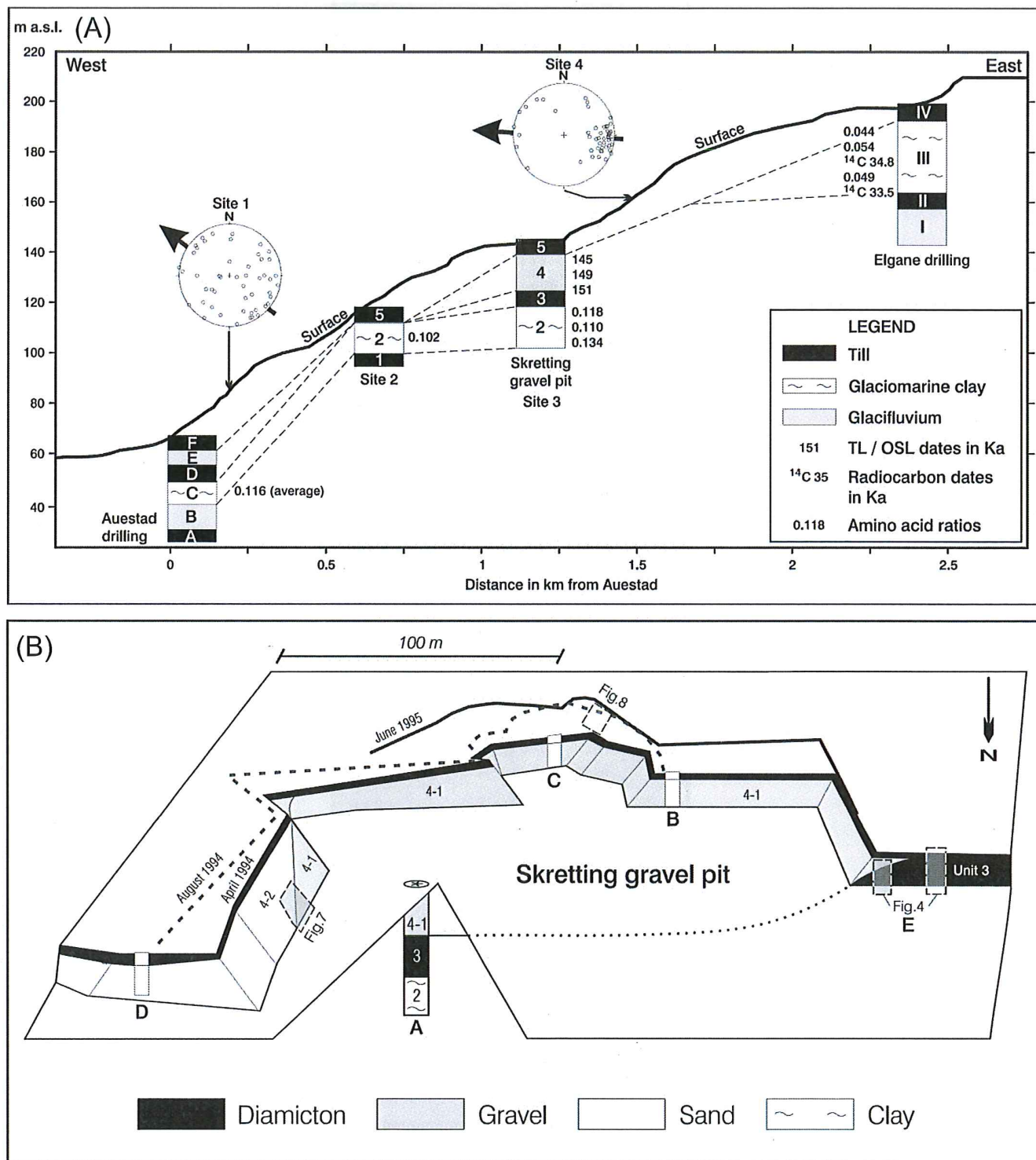


Fig. 18. (A) E-W profile crossing the southern part of the Jæren escarpment showing correlation of units between investigated sites. Stratigraphy from Auestad and Elgane taken from Janocko et al. (1998). Clast fabric analysis in tills from sites 1 and 4 are plotted on a Schmidt net lower hemisphere. Arrows show interpreted ice-flow directions. Note the vertical exaggeration. (B) Sketch of the Skretting gravel pit seen from the north. Photographs, sites for drilling (A) and detailed logging (B, C and D) are indicated. From Stalsberg et al. (1999).

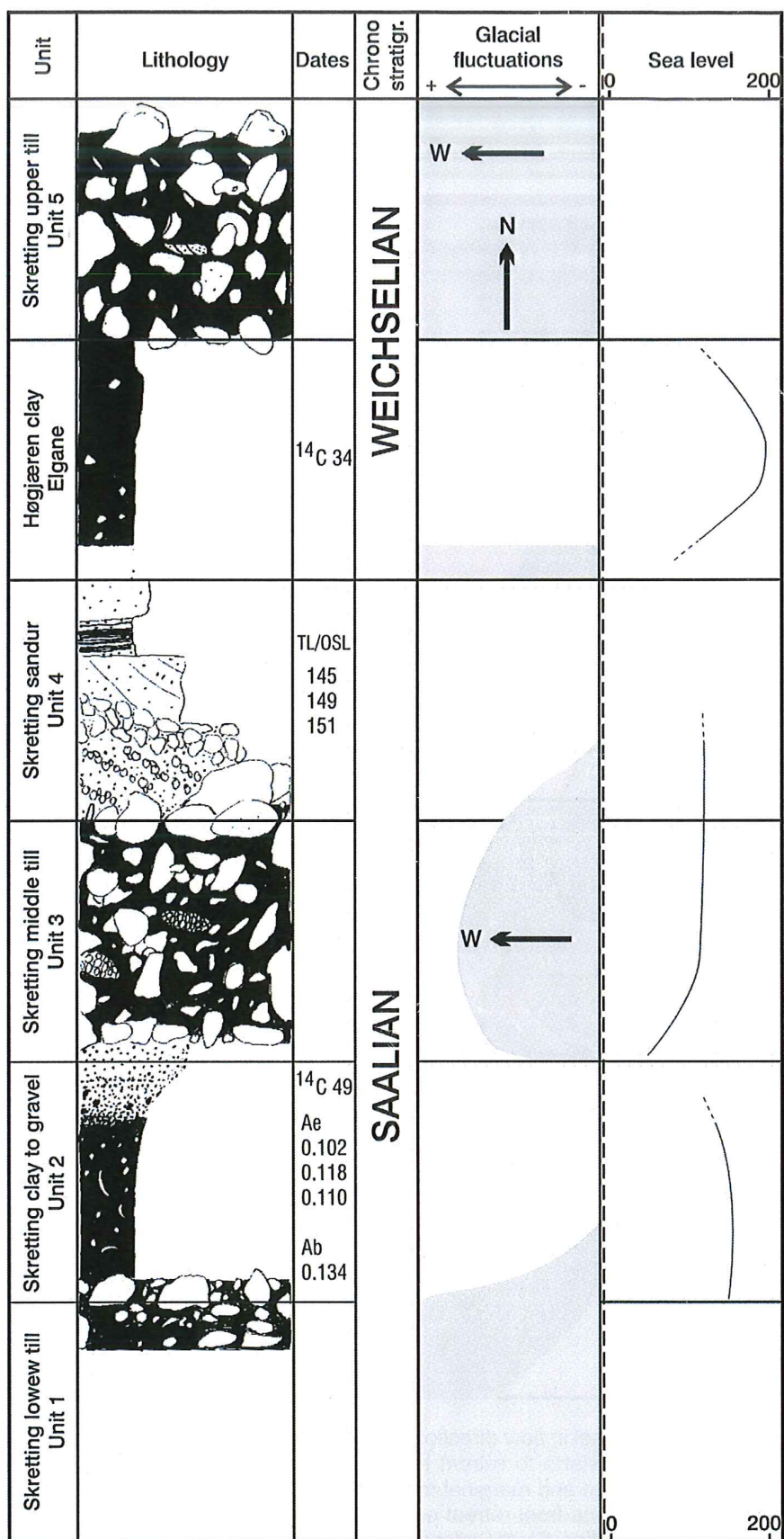


Fig. 19. Composite stratigraphy of the Skretting area. Relative sea-level is indicated. Arrows show suggested ice-flow direction. Ae and Ab indicate amino acid ratios from *Elphidium excavatum* and *Bulimina marginata* respectively. Data from the Høgjæren clay are derived from Janocko et al. (1998). Figure taken from Stalsberg et al. (1999).



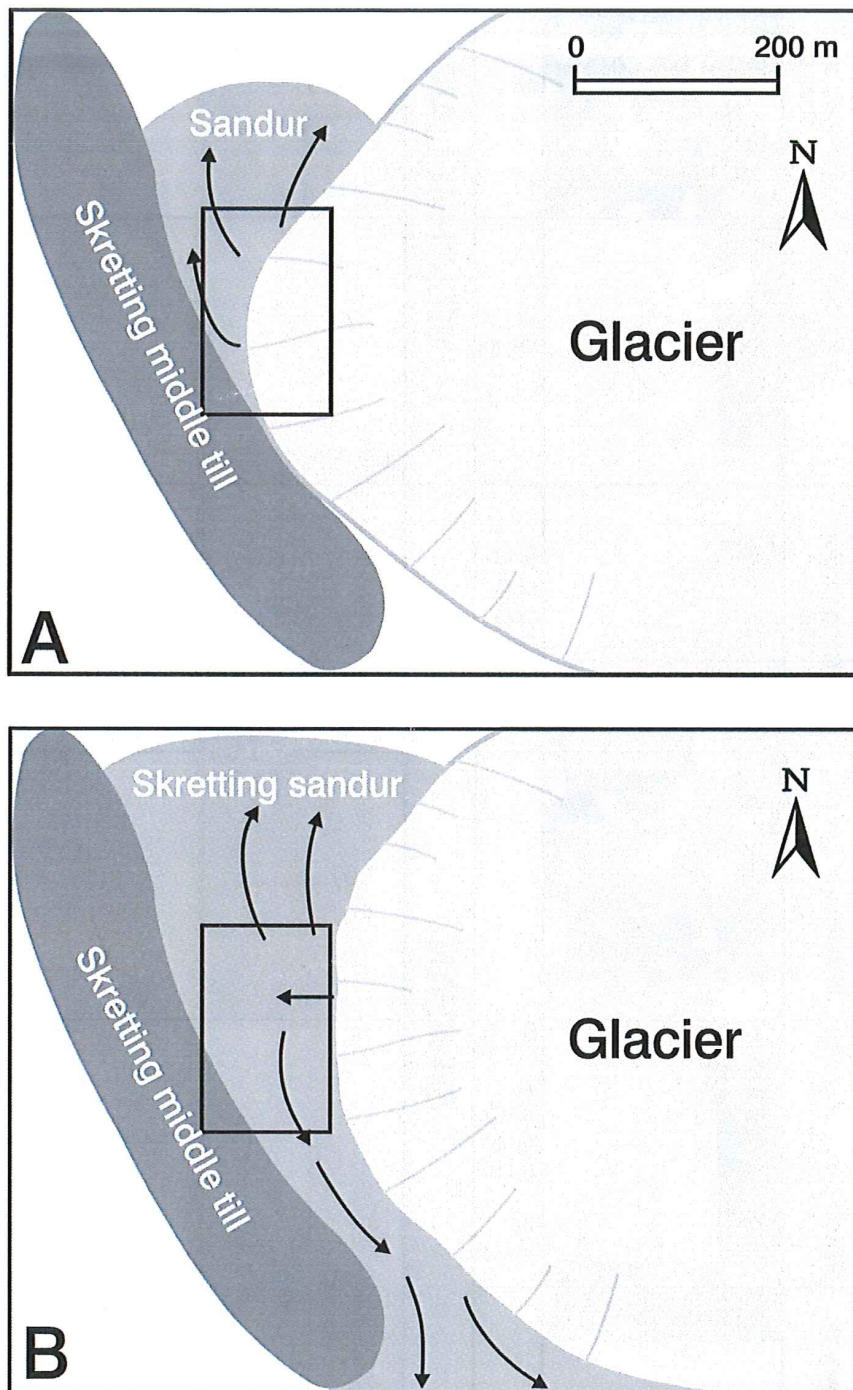


Fig. 20. The reversal in flow direction during formation of Skretting sandur. (A) The glacier front starts to retreat leaving space for sediment accumulation between ice margin and marginal moraine and directs meltwater towards the north. (B) Further ice-front retreat provides an opening towards the south and changes flow direction. From Stalsberg et al. (1999).

## Site 6: Elgane

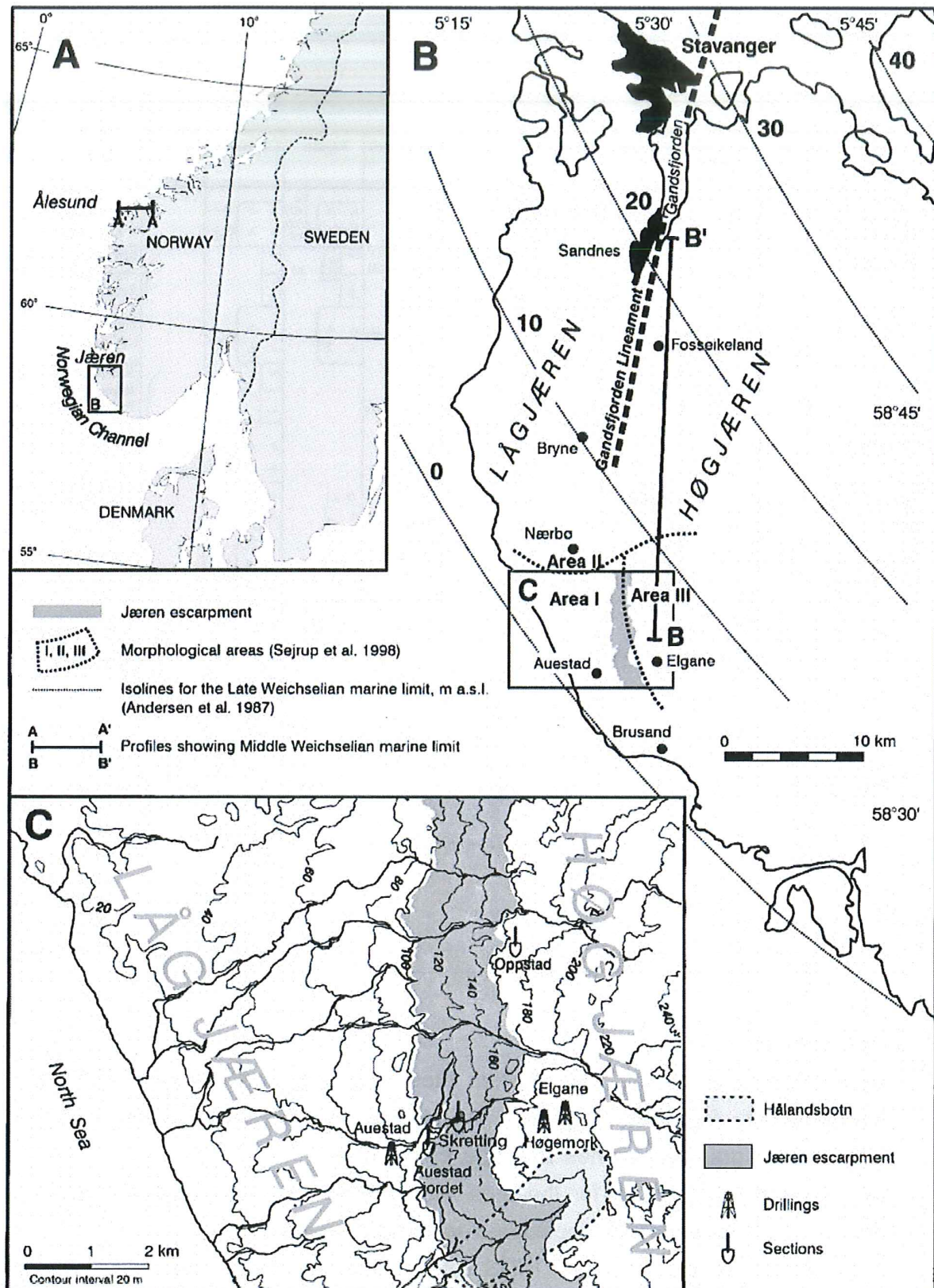


Fig. 21 Study area and names mentioned in the text.

A Part of southern Scandinavia with localization of Jæren and the Norwegian Channel.

B Zoom on the Jæren area showing: the main geological features in the region (Grandsfjorden Lineament – dashed line, Jæren escarpment separating Low Jæren to High Jæren – grey), the division of the three different morphological regions in southern Jæren according to *Sejrup et al.* (1998) (Areas I to III), the Late Weichselian marine limit isobases after *Andersen et al.* (1987), and the drill sites of Auestad and Elgane.

C Details of the study area with the two drill sites presented in the paper and other sites discussed in the text. From *Larsen et al.* (2000).





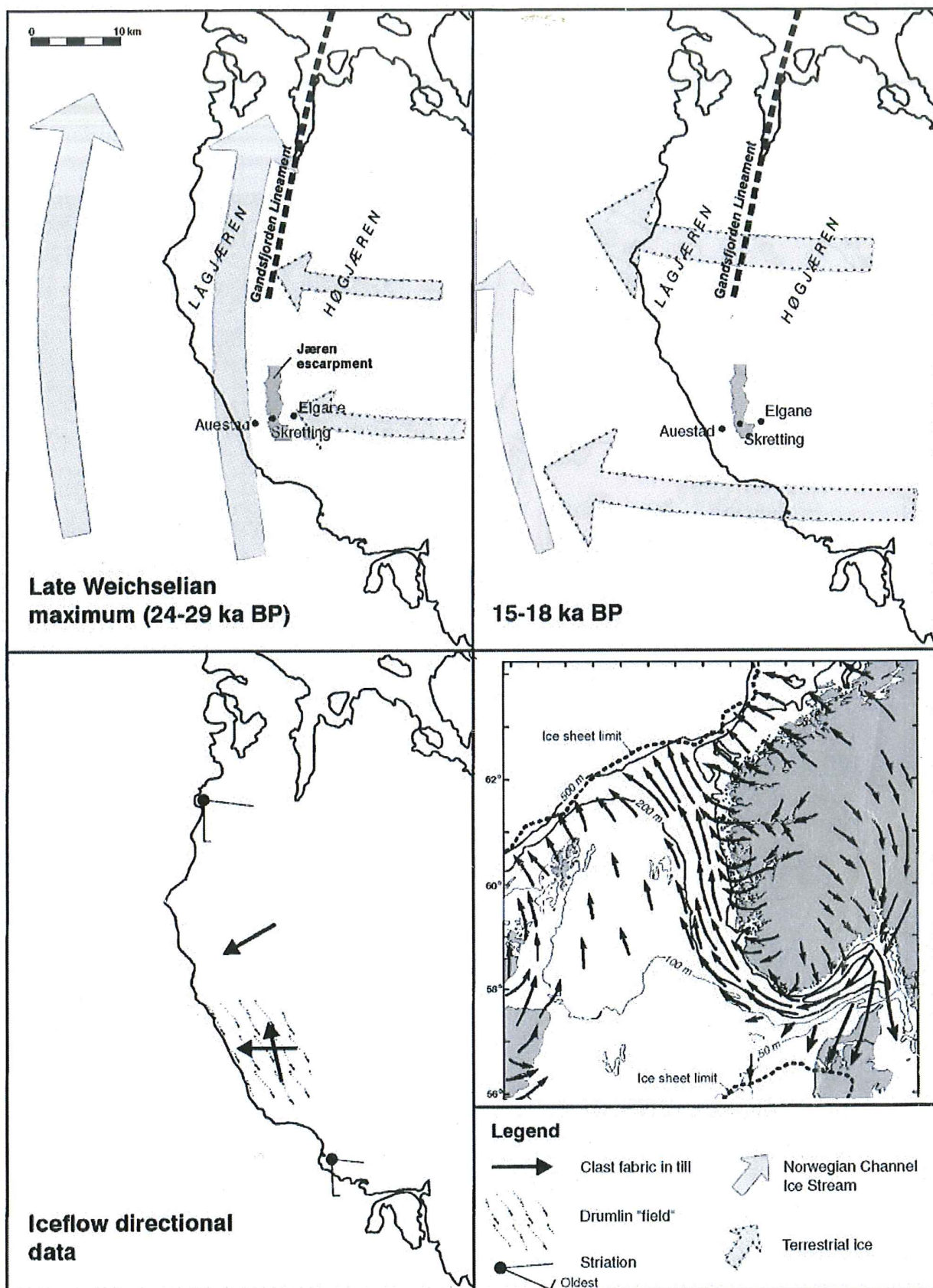


Fig. 23 Interaction between the NCIS across Jæren at the last glacial maximum (top left corner) and during a glacier advance across the coastline by terrestrial-based ice about 18-15 ka ago, as the ice stream calved back in the Norwegian Channel (top right corner). The bottom left corner shows some ice flow directional data from areas below the Jæren escarpment. The bottom right map shows a more regional picture of the ice flow during a maximum-type glaciation (modified from Sejrup *et al.* (1998)).



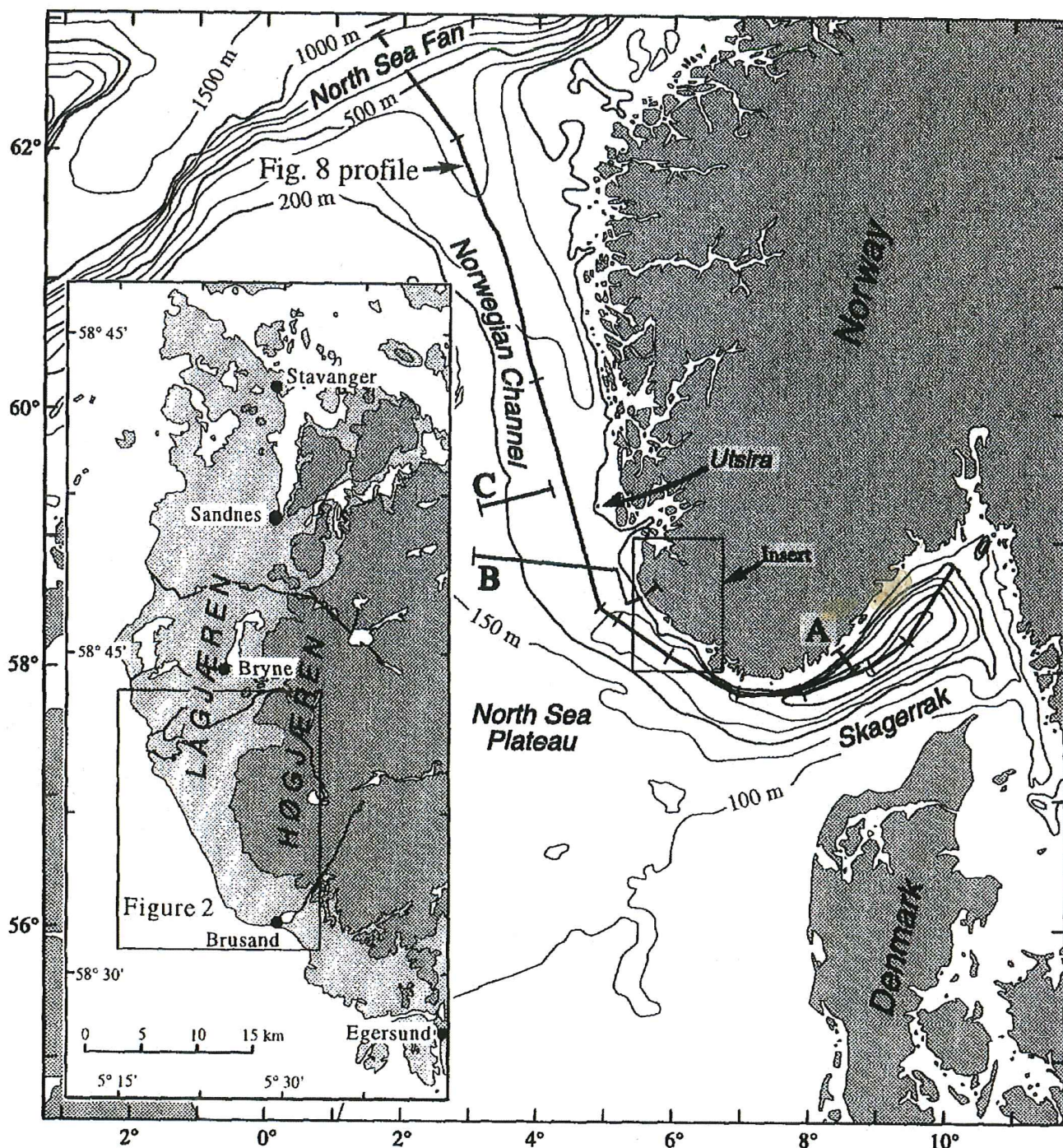


Fig. 24. Map of western Norway, the Norwegian Channel and Jæren (inset with darker shading 200 m a.s.l.). From Sejrup et al. (1998).



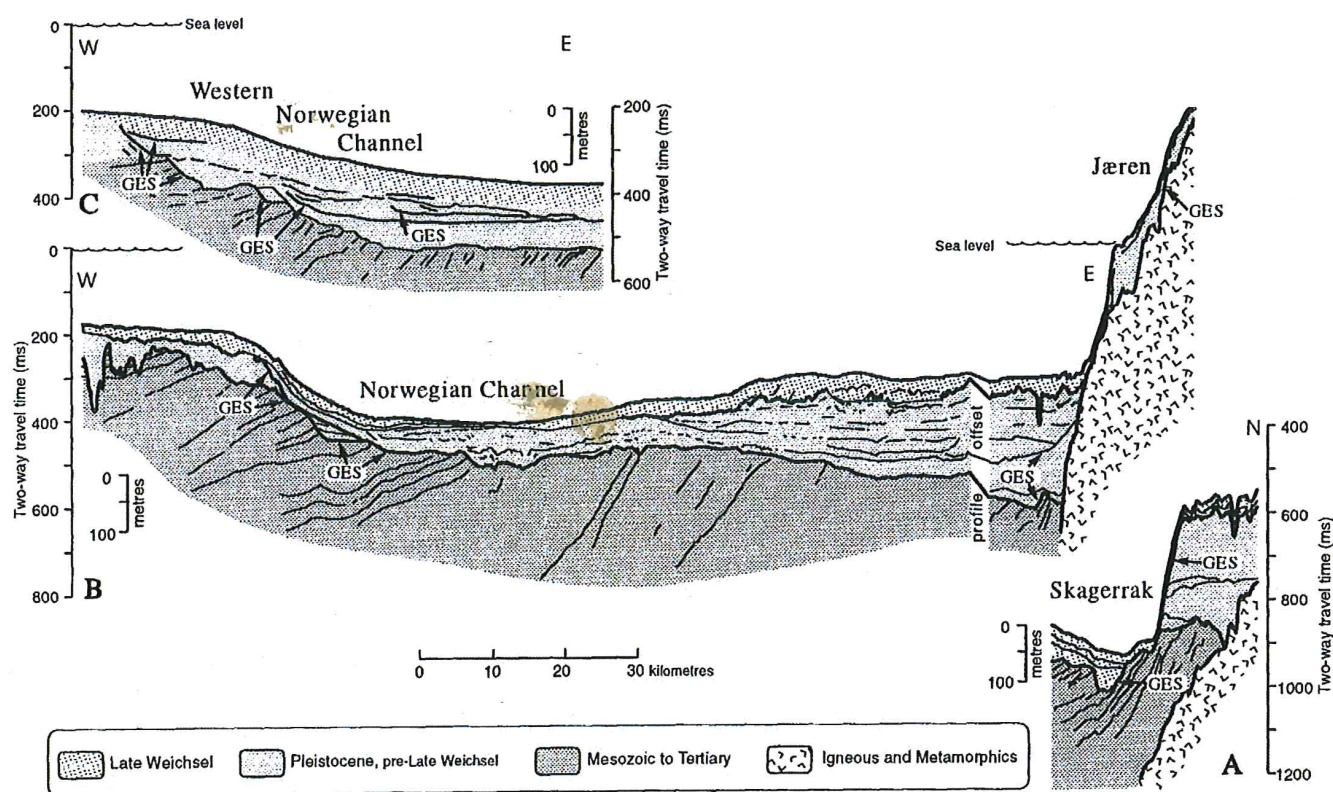


FIG. 25. Cross sections (seismic interpretations) of the Norwegian Channel (for location see Fig. 24). Numerous generations of 'U'-shaped or half-'U'-shaped erosion scarps from Channel-parallel ice stream flow are indicated (GES). Marine/glaciomarine deposits constitute a small portion of the deposits (parallel stratification). The thick Quaternary erosional remnants in profile A (redrawn from Haugwitz and Wong, 1993) are a larger scale analogue to Jæren deposits. From Sejrup et al. (1998).



## Day 2 excursion

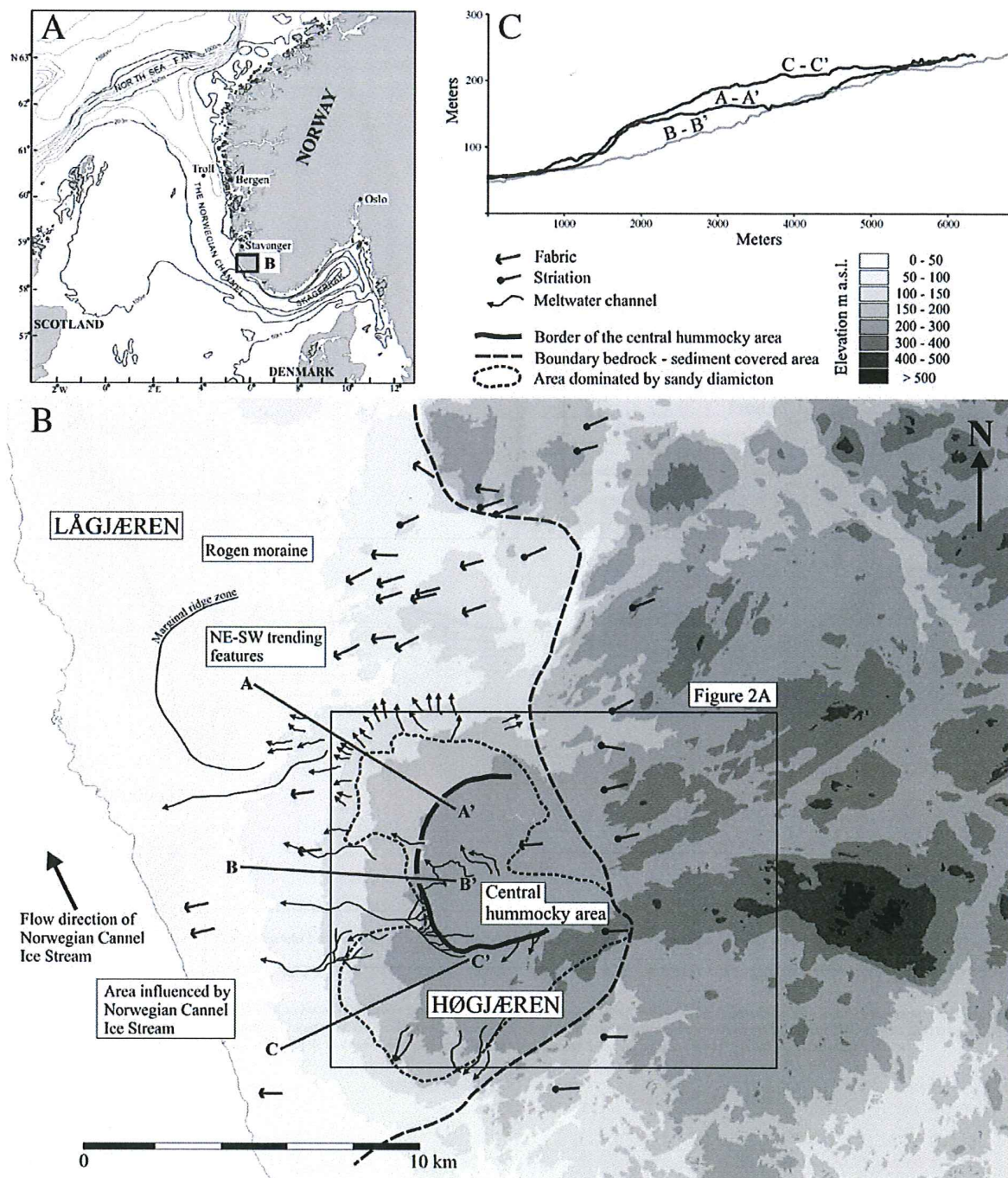


Fig. 26 (A) Overview map showing the location of the study area Jæren (within box), adjacent to the Norwegian Channel. (B) Map of the southern part of Jæren showing the location of the Høgjæren plateau and the sharp delineation between sediment covered areas to the west and bedrock dominated areas to the east and south. The distribution of sandy diamicton on the Høgjæren plateau is also shown. Striations and fabric measurements (Andersen et al., 1987), which show that the last ice movement was towards SW. Meltwater channels (mainly after Andersen et al., 1987), display a radial pattern from the central Høgjæren plateau. Profiles A-C are presented in C. (C) Topographical profiles from Lågjæren to Høgjæren show an even and gentle western slope and a more stepwise northern and southern slope. From Knudsen et al. (2006).



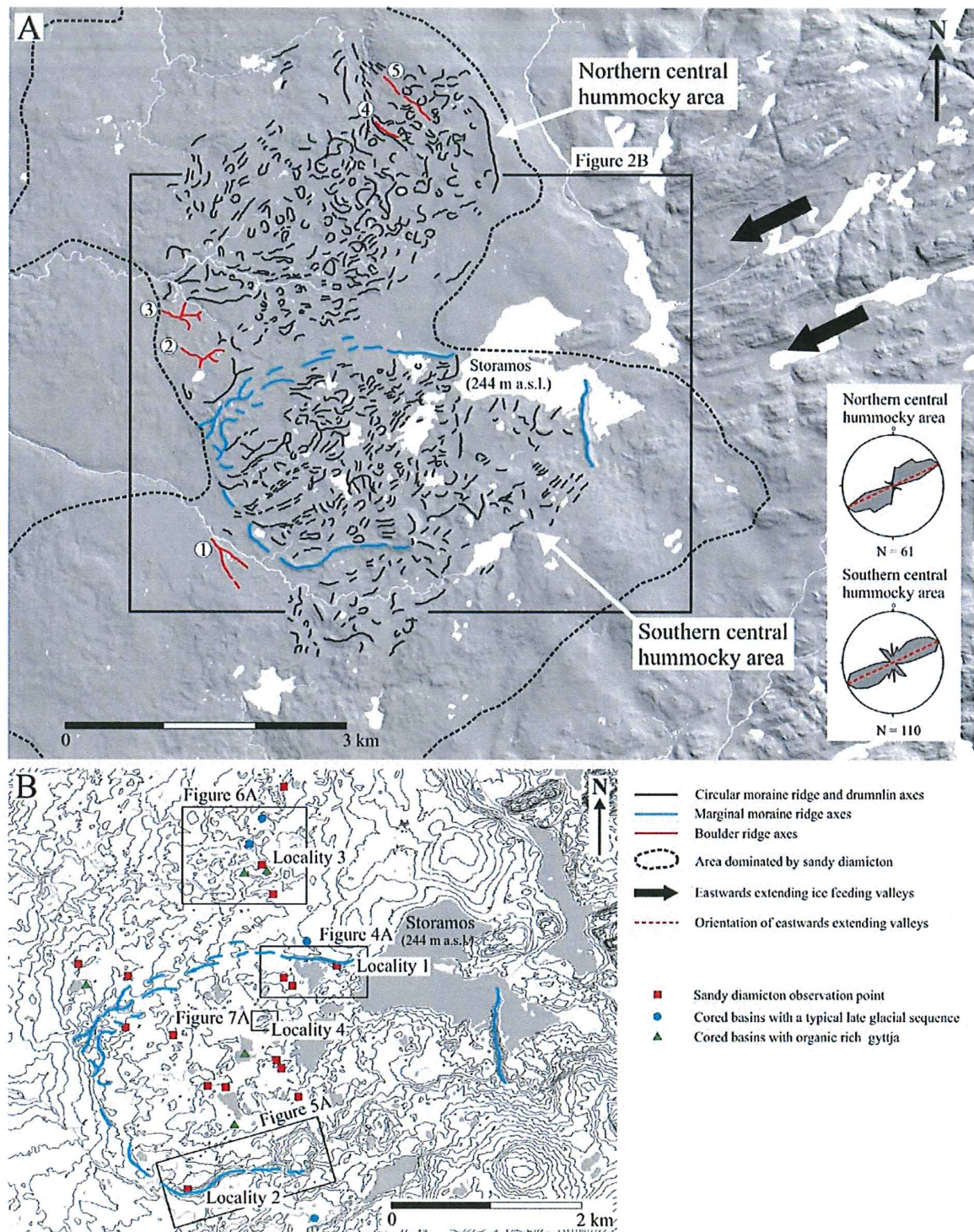


Fig. 27. (A) Digital elevation model of the Høgjæren plateau and the bedrock area to the east. Ridge axes in the central hummocky area are drawn from air photographs and marked as lines. 2D rose diagrams, presenting orientation of the long axis of straight crested ridges N50 m long, show orientation parallel to the last known ice movement in the area and to the valleys extending eastwards. Orientation of the valleys is marked with a red stippled line on the rose diagrams. Note also that the most of the open lakes are situated in the southern area. (B) Topographical map, with equidistance 5 m, showing localities where sandy diamicton has been observed in sections and locations of basins cored with a Russian peat corer. Machine-dug excavations have been investigated at Localities 1–3. From Knudsen et al. (2006).



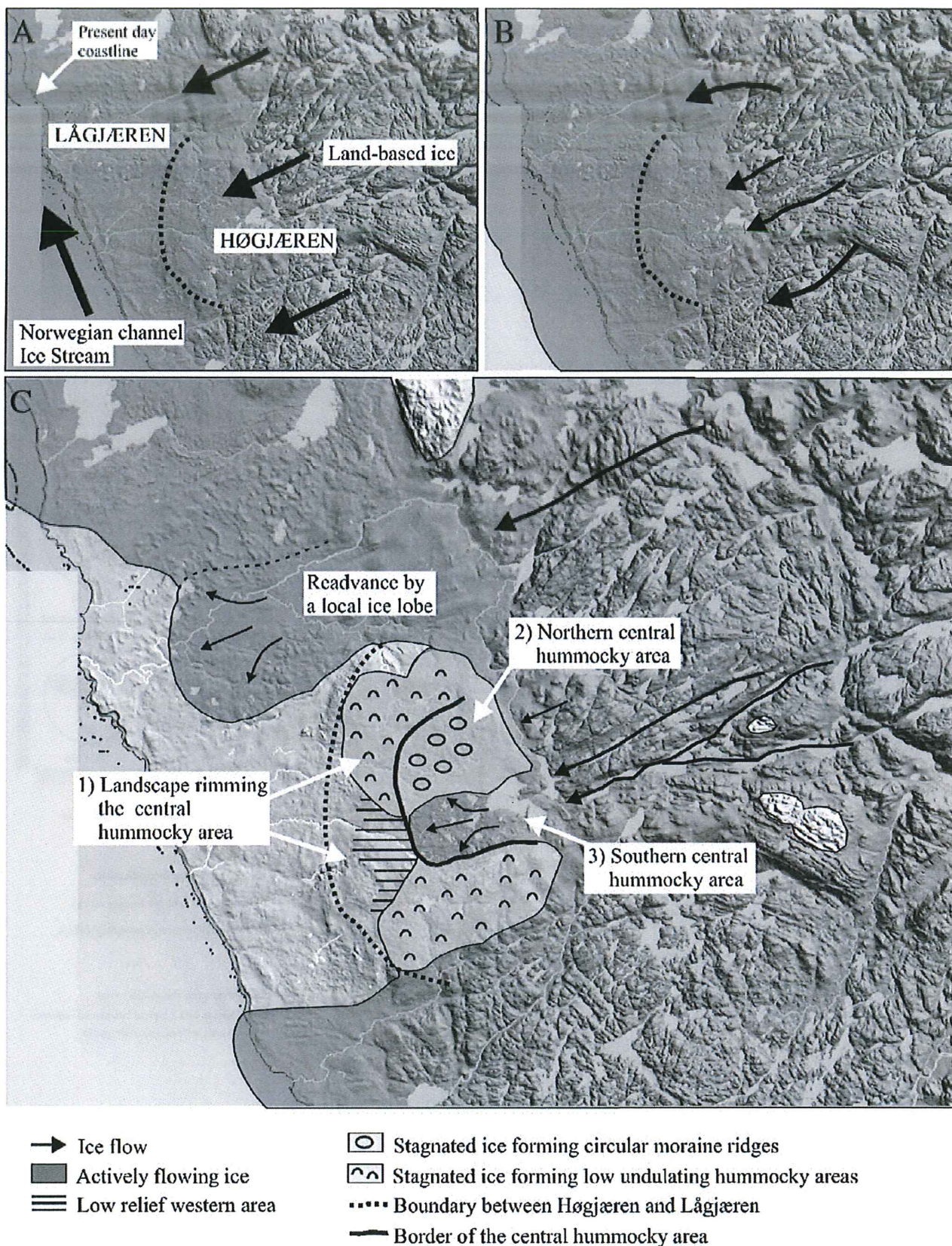
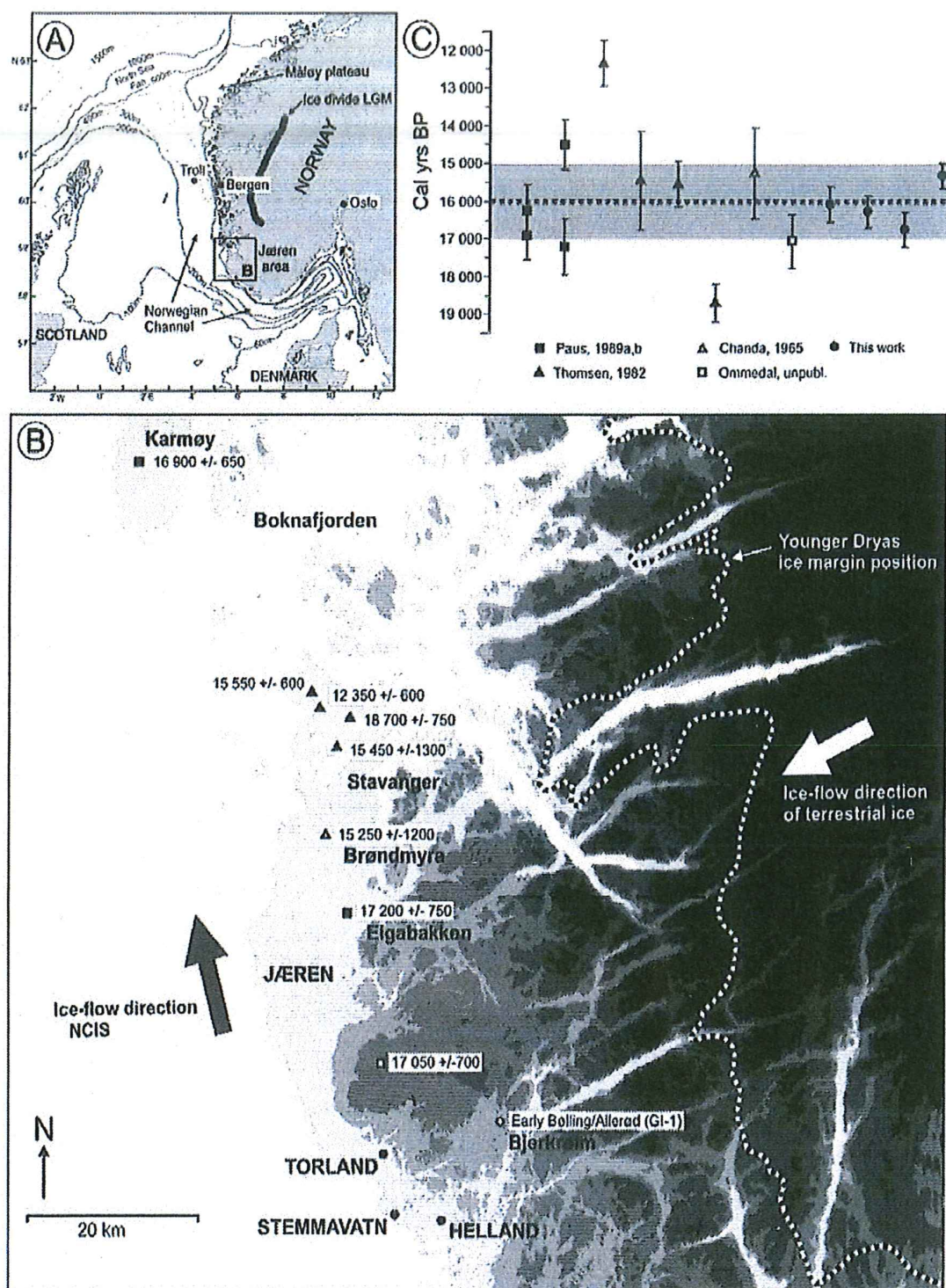


Fig. 28. Ice dynamic model for the last deglaciation on southern Jæren. The border between Lågjæren and Høgjæren is drawn at approximately 120 m a.s.l. Relative ice flow is illustrated by relative sizes of arrows. The stagnated ice probably appeared patchy and not as a continuous cover. (A) At glacial maximum is the Norwegian Channel Ice Stream (NCIS) flowing northwards in the Norwegian Channel, inundating the western part of Lågjæren. Land-based ice is feeding into the ice stream. (B) Rapid disintegration of the NCIS causes a dynamical readvance of the land-based ice beyond the present coast line and a subsequent lowering of the ice surface (Raunholm et al., 2003). The flow of ice is probably deflected to the north and south sides of the Høgjæren plateau. This limits the supply of material to Høgjæren and areas west of the plateau during this phase. (C) The ice stagnates to the north and south of the central hummocky area. Continuous flow of ice supplies sandy material to the central part of the Høgjæren plateau and drumlins are probably formed. Ice in the northern central area stagnates due to the lack of ice-feeding channels, and circular moraine ridges and glaciofluvial features form in this stagnated glacial regime. Ice flow is either kept active or reactivated in the southern central area causing formation of marginal moraine ridges surrounding an area dominated by drumlins. The area influenced by a readvance of a local ice lobe at Lågjæren is mapped by Raunholm et al. (2003). Taken from Knudsen et al. (2006).





**Fig. 29.** A. Overview map of south Norway and the North Sea area, with the location of the study area. The bathymetry of the Norwegian Channel, the location of the Troll site, the Måløy plateau and the main ice divide during the last glacial maximum (LGM) are marked. B. Map of the Jæren area, with locations of the Torland, Stemnavatn and Helland sites marked. Previously investigated basins and the respective bottom dates, representing minimum ages for deglaciation, are also shown. All ages are in cal yrs BP, calibrated with OxCal v3.10 (Bronk Ramsey 2001, 2005), with the atmospheric data IntCal04 (Reimer *et al.* 2004). Ice flow directions of the Norwegian Channel Ice Stream (NCIS) and terrestrial ice from central S Norway and the Younger Dryas (GS-1) ice margin position according to Andersen *et al.* (1987) is also shown. C. Calibrated ages of bottom dates on mainly bulk sediment samples and aquatic moss from the Jæren area. The symbol denoting the dates corresponds to the symbols that mark the localities in A. The gray shaded time span shows a reasonable estimate for the timing of deglaciation in the Jæren area; between 17 000 and 15 000 cal yrs BP. Knudsen *et al.* (in prep).



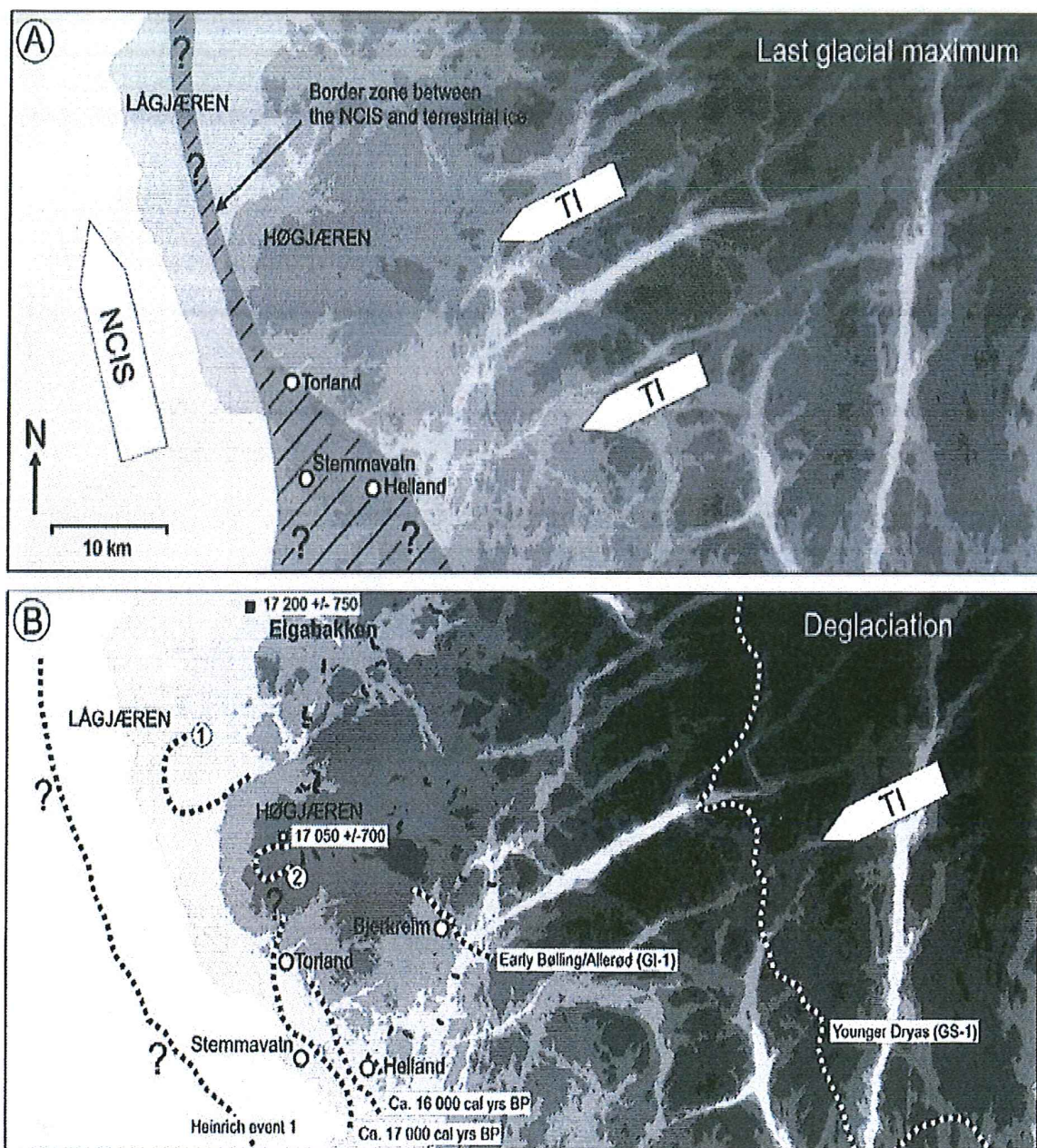


Fig. 30. (A) The ice extent during the last glacial maximum in the Jæren area. The border zone between the northwards flowing Norwegian Channel Ice Stream (NCIS) and the terrestrial ice was situated east of the present coastline, but was displaced westwards beyond the coastline when the NCIS collapsed (Sejrup *et al.* 1998; Larsen *et al.* 2000; Raunholm *et al.* 2003). The NCIS offshore of the Jæren area disintegrated prior to ca. 17 600 cal yrs BP. (B) Ice marginal positions at different times during retreat of the terrestrial ice in the Jæren area shown by stippled lines. The marginal positions are approximate and based on the data presented in this paper in addition to data from (Andersen *et al.* 1987; Ommedal, unpubl. data; Paus 1989a; Paus 2003; Raunholm *et al.* 2003; Knudsen *et al.* 2006). 1) and 2) show the ice marginal advances mapped by Raunholm *et al.* (2003) and Knudsen *et al.* (2006) respectively. The small black lines are proglacial deposits as mapped by Andersen *et al.* (1987). From Knudsen *et al.* (in prep.)



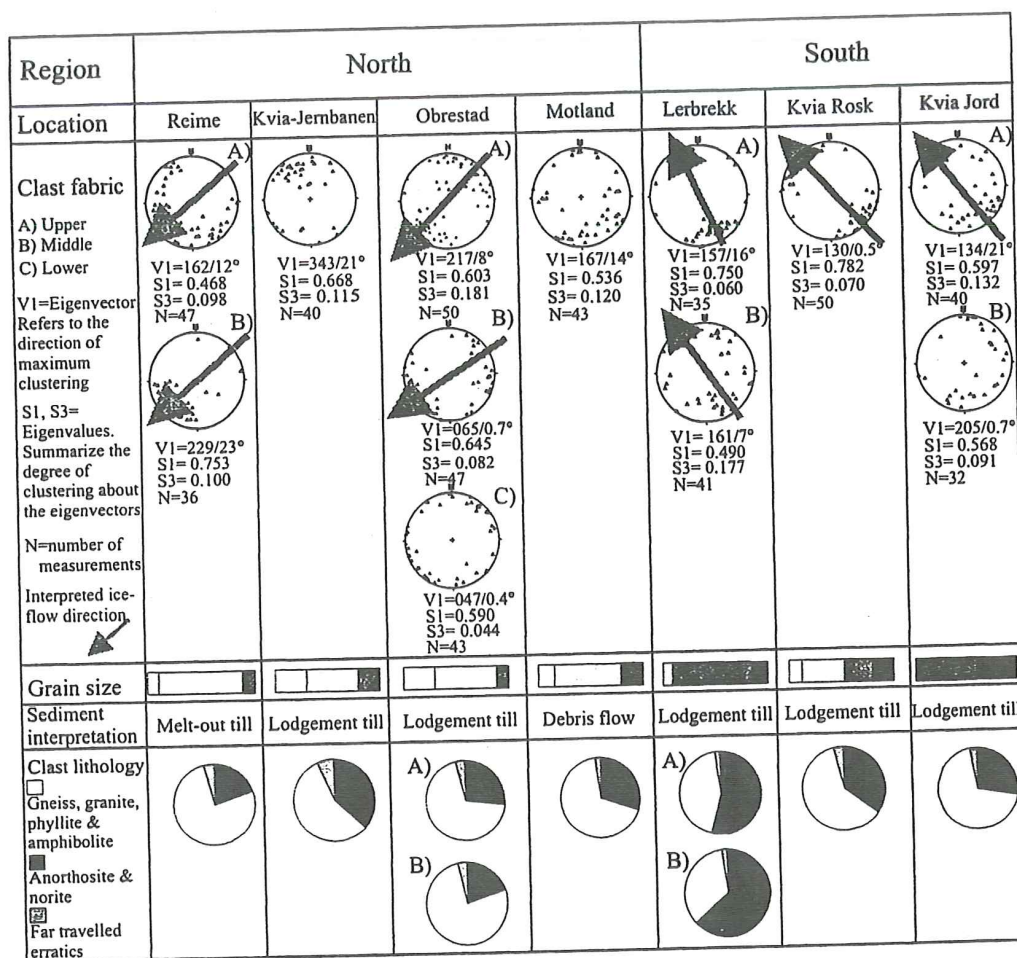


Fig. 7. Diagram showing clast fabric data, clast lithologies, interpreted ice-flow direction, genetic interpretation of the upper diamicton and grain size of till matrix (white = gravel, light grey = sand, dark grey = silt, black = clay).

till (Fig. 7) (Dreimanis 1989). Because of a uniform lithology and stratigraphical position, the till at all sites in the southern region is considered to be contemporaneous. Deformation of sub-till glaciofluvial and glaciolacustrine sediments indicates ice-flow towards the north during till deposition (Stalsberg, unpublished data).

#### Northern region: gravel-rich diamicton

Four sections were studied in the northern region; Reime, Kvia-Jernbanen, Obrestad and Motland (Fig. 3). The uppermost unit at all sections is a 1.5–4 m thick gravel-sand rich diamicton, overlying

glaciofluvial and/or glaciolacustrine sediments (Fig. 6).

The Obrestad, Reime and Kvia-Jernbanen sites are considered to evidence lobe-formed marginal moraines (Fig. 3). The two former sites differ morphologically from the Kvia-Jernbanen site as the sections are in ridges. The Obrestad section is in a remnant of a ridge and the section has recently been described by Janocko (1997), who interpreted the former ridge to be a drumlin deposited by a NW flowing glacier and later overridden by a SW flowing glacier.

The uppermost diamicton at Obrestad and the one at Kvia-Jernbanen are very similar (Fig. 6). At both sites the diamicton is matrix-supported and

has a sharp and erosive lower boundary. The size of the matrix varies and upward from silt and fine sand to medium to coarse sand and gravel. Clast content increases upward. The clasts have a light brown to dark brown colour, are mainly sub-rounded with only angular and angular. Some are striated. The upper 2 m of Kvia-Jernbanen is stratified (Fig. 7). This stratification results from pebbles and cobbles into horizontal layers with a low dip to NNW. Based on the erosive nature of the massive and compact lower clasts, the diamicton is in lodgement till (Fig. 7) (Dreimanis 1989). However, stratification in the upper part of the till has been influenced by ice flow. The diamicton at Obrestad is interpreted by Janocko (1997) to be a till.

The upper diamicton at Kvia-Jernbanen is approximately 1.8 m thick (Fig. 6). It is matrix- and clast-supported, brown colour. The matrix is sand. Clasts inside the whole unit are rounded and the maximum diameter is 10 cm. Boulder frequency is high in the eastern part of the section. There is some occurrence of some very large boulders in the upper part of the unit. The stratification and there is a general clustering of some boulders with an 18° dip towards E enhanced by some boulders long axes showing the same dip. The unit has a high frequency of unsorted lenses and intrabeds. The intrabeds consist of very fine sand and silt mainly lying above boulders and cobbles showing lamination.

The diamicton is interpreted to be a till (Fig. 7) (Dreimanis 1989, 1990). This is based on vertical combination with sorted intrabeds thought to be till processes. This interpretation is supported by vague stratification and the presence of boulders and cobbles into bands which from stratified englacial deposits where primary sedimentary structures are commonly found.



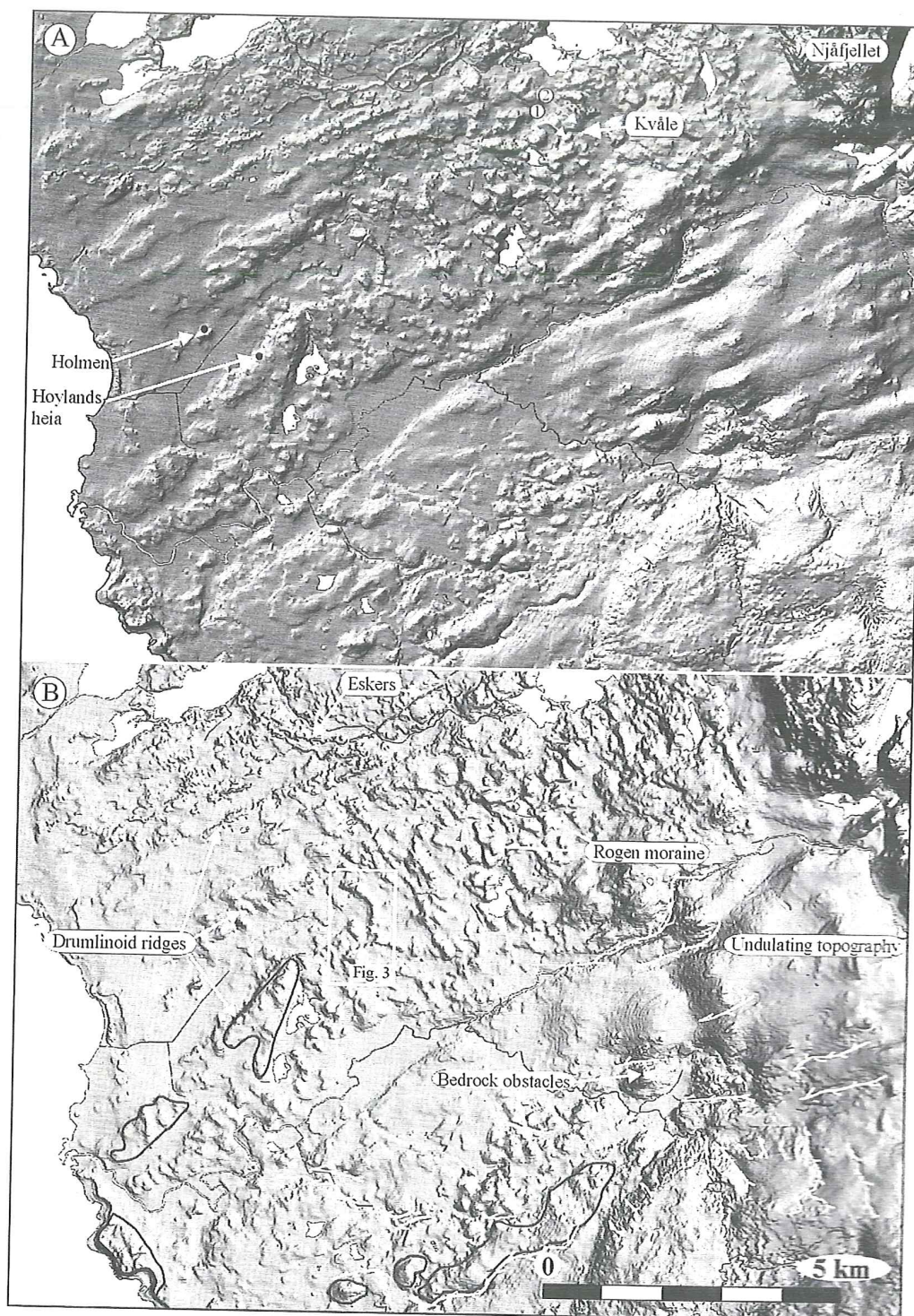


Fig. 2. Geomorphology of the Bryne/Nærbø area (Fig. 1). A and B show the same area, but with different hill shading. A. The hill shade is from the northwest, highlighting NE-SW trending features (e.g. eskers and drumlinoid ridges in the northern part of the figure). Numbers 1–2 mark the two investigated ridges at Kvåle. B. The illumination is from the northeast, and ridges transverse to this are highlighted. White lines mark the most pronounced meltwater channels. Black circles mark ridges interpreted as marginal moraines by Sejrup *et al.* (1998), Jónsdóttir *et al.* (1999) and Stalsberg (2000).

### Acknowledgments

GLANAM is an ITN project and has received funding from the People Programme (Marie Curie Actions) of the European Union's Seventh Framework Programme FP7/2007-2013/ under REA grant agreement n° 317217.

